1166 *Inorg. Chem.* **2010**, *49*, 1166–1179
DOI: 10.1021/ic9021323

Inorganic Chemistry
Article

Anionic Amino Acid [*closo*-1-CB_9H_8-1-COO-10-NH_3]$^-$ and Dinitrogen Acid [*closo*-1-CB_9H_8-1-COOH-10-N_2] as Key Precursors to Advanced Materials: Synthesis and Reactivity†

Bryan Ringstrand,‡ Piotr Kaszynski,*,‡ Victor G. Young, Jr.,§ and Zbynek Janoušek∥

‡*Organic Materials Research Group Department of Chemistry, Vanderbilt University, Nashville, Tennessee 37235,* §*Crystallographic Laboratory, Department of Chemistry, University of Minnesota, Twin Cities, Minnesota 55455, and* ∥*Institute of Inorganic Chemistry, Academy of Sciences of the Czech Republic, 250 68 Řež, Czech Republic*

Received October 27, 2009

Amino acid [*closo*-1-CB_9H_8-1-COO-10-NH_3]$^-$ (**4**) was prepared by amination of iodo acid [*closo*-1-CB_9H_8-1-COOH-10-I]$^-$ (**1**) with LiHMDS in a practical and reproducible manner. The apparent dissociation constants, pK_2 = 5.6 and pK_1 > 11, were measured for **4**[**NMe$_4$**] in 50% aq. EtOH. Diazotization of **4** with $NO^+PF_6^-$ under mildly basic conditions afforded stable dinitrogen acid [*closo*-1-CB_9H_8-1-COOH-10-N_2] (**5**). Activation parameters ($\Delta H^{\ddagger}$ = 33.9 ± 1.4 kcal mol^{-1} and $\Delta S^{\ddagger}$ = 10 ± 3.5 cal mol^{-1} K^{-1}) for thermolysis of its methyl ester [*closo*-1-CB_9H_8-1-COOMe-10-N_2] (**11**) in PhCN were established, and the heterolysis of the B−N bond is believed to be the rate-determining step. Electrochemical analysis showed a partially reversible reduction process for **11** ($E_{1/2}^{red}$ = −1.03 V) and **5**$^-$ ($E_{1/2}^{red}$ = −1.21 V), which are more cathodic than reduction of [*closo*-1-CB_9H_9-1-N_2] (**17**). The dinitrogen acid **5** was reacted with pyridine and *N*,*N*-dimethylthioformamide, to form pyridine acid **6** and protected mercapto acid **7**, respectively, through a boronium ylide intermediate **18**. Compound **7** was converted to sulfonium acid **8**. The molecular and crystal structures for **5** [$C_2H_9B_9N_2O_2$ monoclinic, $P2_1/n$, a = 7.022(2) Å, b = 11.389(4) Å, c = 12.815(4) Å, β = 96.212(5)°; V = 1018.8(6) Å^3, Z = 4,], **6** [$C_7H_{14}B_9NO_2$, monoclinic, $P2_1/n$, a = 14.275(4) Å, b = 12.184(3) Å, c = 30.538(8) Å, β = 95.377(4)°; V = 5288(3) Å^3, Z = 16], and **8** [$C_7H_{19}B_9O_2S$, monoclinic, $P2_1/c$, a = 15.988(5) Å, b = 19.377(6) Å, c = 9.655(3) Å, β = 98.348(5)°; V = 2959.4(16) Å^3, Z = 8] were determined by X-ray crystallography and compared with results of density functional theory (DFT) and MP2 calculations. Electronic structures of **5**, **6**, and related species were elucidated with electronic spectroscopy and assessed computationally at the B3LYP/6-31G(d,p), MP2/6-31G(d,p), and ZINDO//MP2 levels of theory.

Introduction

closo-Carbaborates[1,2] [*closo*-1-CB_9H_{10}]$^-$ (**A**)[3] and [*closo*-1-$CB_{11}H_{12}$]$^-$ (**B**)[4,5] (Figure 1) are becoming increasingly important building blocks for advanced materials such as ionic liquids,[6] lithium ion battery electrolytes,[7] ionic liquid crystals,[8] polar liquid crystals,[9] nonlinear optical (NLO) materials,[10] and also agents for Boron Neutron Capture Therapy[11−13] (BNCT) and Photodynamic Therapy[11,14,15] (PDT). The attractiveness

† Dedicated to Professor Josef Michl on the occasion of his 70th birthday.

*To whom correspondence should be addressed. E-mail: piotr.kaszynski@vanderbilt.edu. Phone: (615) 322-3458. Fax: (615) 343-1234.

(1) Stibr, B. *Chem. Rev.* **1992**, *92*, 225–250.
(2) Sivaev, I. B.; Kayumov, A.; Yakushev, A. B.; Solntsev, K. A.; Kuznetsov, N. T. *Koord. Khim.* **1989**, *15*, 1466–1477.
(3) Nestor, K.; Stibr, B.; Kennedy, J. D.; Thornton-Pett, M.; Jelinek, T. *Collect. Czech. Chem. Commun.* **1992**, *57*, 1262–1268.
(4) Körbe, S.; Schreiber, P. J.; Michl, J. *Chem. Rev.* **2006**, *106*, 5208–5249.
(5) Michl, J. *Pure Appl. Chem.* **2008**, *80*, 429–446.
(6) Larsen, A. S.; Holbrey, J. D.; Tham, F. S.; Reed, C. A. *J. Am. Chem. Soc.* **2000**, *122*, 7264–7272. Nieuwenhuyzen, M.; Seddon, K. R.; Teixidor, F.; Puga, A. V.; Viñas, C. *Inorg. Chem.* **2009**, *48*, 889–901.
(7) Ivanov, S. V.; Casteel, W. J.; Bailey, W. H. *U.S. Patent Appl.* **2007**, US 2007189946. Pez, G. P.; Ivanov, S. V.; Dantsin, G.; Casteel, W. J.; Lehmann, J. F. *Eur. Patent Appl.* **2007**, EP 1763099.
(8) Ringstrand, B.; Kaszynski, P.; Monobe, H. *J. Mater. Chem.* **2009**, *19*, 4805–4812.
(9) Ringstrand, B.; Kaszynski, P.; Young, V. G., Jr.; Januszko, A. *J. Mater. Chem.* **2009**, *19*, 9204–9212.
(10) Grüner, B.; Janousek, Z.; King, B. T.; Woodford, J. N.; Wang, C. H.; Vsetecka, V.; Michl, J. *J. Am. Chem. Soc.* **1999**, *121*, 3122–3126.
(11) Sivaev, I. B.; Bregadze, V. V. *Eur. J. Inorg. Chem.* **2009**, 1433–1450.
(12) Wilbur, D. S.; Hamlin, D. K.; Srivastava, R. R.; Chyan, M.-K. *Nucl. Med. Biol.* **2004**, *31*, 523–530.
(13) Sivaev, I. B.; Bregadze, V. I.; Kuznetsov, N. T. *Russ. Chem. Bull., Int. Ed.* **2002**, *51*, 1362–1374.
(14) Ol′shevskaya, V. A.; Zaitsev, A. V.; Luzgina, V. N.; Kondratieva, T. T.; Ivanov, O. G.; Kononova, E. G.; Petrovskii, P. V.; Mironov, A. F.; Kalinin, V. N.; Hofmann, J.; Shtil, A. A. *Bioorg. Med. Chem.* **2006**, *14*, 109–120.
(15) Ol′shevskaya, V. A.; Nikitina, R. G.; Zaitsev, A. V.; Luzgina, V. N.; Kononova, E. G.; Morozova, T. G.; Drozhzhina, V. V.; Ivanov, O. G.; Kaplan, M. A.; Kalinin, V. N.; Shtil, A. A. *Org. Biomol. Chem.* **2006**, *4*, 3815–3821.

Published on Web 12/31/2009

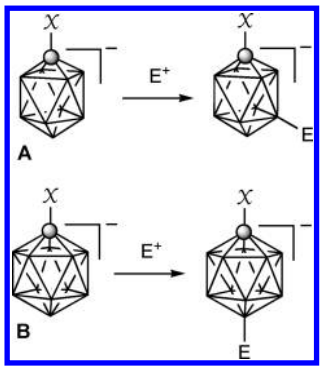

Figure 1. Substitution pattern in carbaborates **A** and **B**. Each vertex represents a BH fragment, and the sphere is a carbon atom.

of these clusters stems largely from their electronic features which are manifested in complete charge delocalization, low nucleophilicity,[16] and chemical stability under ambient conditions because of sigma-aromaticity of the skeleton.[1,4,17,18] In BNCT and PDT applications, the lipophilic nature of these anions assists otherwise hydrophobic molecules to cross cellular membranes in biological systems. On the other hand, the geometry of the clusters is suitable for the construction of anisometric molecules[19] as has been demonstrated for their electrically neutral carborane analogues.[20−27]

The 12-vertex carbaborate, $[closo\text{-}1\text{-}CB_{11}H_{12}]^-$, has been relatively more accessible and many functionalization methods have been devised.[28−31] In contrast, the chemistry of the 10-vertex analogue is less developed in part because of its lesser availability, and in part due to differences in reactivity. For instance, while the electrophilic substitution of the $\{closo\text{-}1\text{-}CB_{11}\}$ cage occurs preferentially at the B(12) position,[10,28,29] the electrophilic attack on the $\{closo\text{-}1\text{-}CB_9\}$ takes place almost exclusively at the B(6) position (Figure 1).[8,32] The inability to form derivatives with substituents in the antipodal positions (the 1,10-disubstitution pattern) was the major obstacle in applications of the $[closo\text{-}1\text{-}CB_9H_{10}]^-$ cluster as a structural element for anisometric molecules and materials such as liquid crystals.

This situation changed when Brellochs discovered[33] a new method for preparing the parent $[closo\text{-}1\text{-}CB_9H_{10}]^-$ and *C*-substitued derivatives.[34−36] The method not only simplified access to the $\{closo\text{-}1\text{-}CB_9\}$ cluster but also permitted the introduction of a substituent at the B(10) position.[37] The next milestone in the chemistry of the $[closo\text{-}1\text{-}CB_9H_{10}]^-$ cluster was the preparation of an isomerically pure 1,10-heterobifunctionalized derivative, the iodo acid **1**.[38] We have demonstrated that the iodine in **1** can be used to introduce alkyl groups in Pd-catalyzed coupling reactions with alkylzinc reagents.[8,9] The COOH group in the iodo acid was transformed to the NH_2 group in amine **2** and subsequently to the stable dinitrogen group, N_2, in **3**.[8] The relatively high stability of the N_2 group at the apical position appears to be general for 10-vertex *closo*-boranes,[39] and several such derivatives of $[closo\text{-}B_{10}H_{10}]^{2-}$ have been prepared and used as intermediates to obtain nitrogen,[40−45] sulfur,[45,46] phosphorus,[47] oxygen,[43,48] and even carbon[43,49] substituted $\{closo\text{-}B_{10}\}$ clusters. Similar stability and synthetic value of the dinitrogen group was recently found for $[closo\text{-}1\text{-}CB_9H_9\text{-}1\text{-}N_2]$; its reactivity is similar to that of benzenediazonium and permits the introduction of heteroatoms at the C(1) position of the cluster.[50] These new findings were exploited in the preparation of the first anion-driven ionic liquid crystals[8] and positive $\Delta\varepsilon$ additives to nematic materials.[9] In contrast, the analogous dinitrogen derivatives of the 12-vertex *closo*-boranes are

(16) Reed, C. A. *Acc. Chem. Res.* **1998**, *31*, 133–139. Strauss, S. H. *Chem. Rev.* **1993**, *93*, 927–942. Krossing, I.; Raabe, I. *Angew. Chem., Int. Ed.* **2004**, *43*, 2066–2090.
(17) King, R. B. *Russ. Chem. Bull.* **1993**, *42*, 1283–1291.
(18) Schleyer, P. v. R.; Najafian, K. *Inorg. Chem.* **1998**, *37*, 3454–3470.
(19) Bullen, N. J.; Franken, A.; Kilner, C. A.; Kennedy, J. D. *Chem. Commun.* **2003**, 1684–1685.
(20) Muller, J.; Base, K.; Magnera, T.; Michl, J. *J. Am. Chem. Soc.* **1992**, *114*, 9721–9722.
(21) Schöberl, U.; Magnera, T. F.; Harrison, R. M.; Fleischer, F.; Pflug, J. L.; Schwab, P. F. H.; Meng, X.; Lipiak, D.; Noll, B. C.; Allured, V. S.; Rudalevige, T.; Lee, S.; Michl, J. *J. Am. Chem. Soc.* **1997**, *119*, 3907–3917.
(22) Yang, X.; Jiang, W.; Knobler, C. B.; Hawthorne, M. F. *J. Am. Chem. Soc.* **1992**, *114*, 9719–9721.
(23) Schwab, P. F. H.; Levin, M. D.; Michl, J. *Chem. Rev.* **1999**, *99*, 1863–1933.
(24) Kaszynski, P.; Douglass, A. G. *J. Organomet. Chem.* **1999**, *581*, 28–38.
(25) Kaszynski, P.; Pakhomov, S.; Tesh, K. F.; Young, V. G., Jr. *Inorg. Chem.* **2001**, *40*, 6622–6631.
(26) Pakhomov, S.; Kaszynski, P.; Young, V. G., Jr. *Inorg. Chem.* **2000**, *39*, 2243–2245.
(27) For other recent publications see: Januszko, A.; Glab, K. L.; Kaszynski, P. *Liq. Cryst.* **2008**, *35*, 549–553. Nagamine, T.; Januszko, A.; Ohta, K.; Kaszynski, P.; Endo, Y. *Liq. Cryst.* **2008**, *35*, 865–884. Januszko, A.; More, K. M.; Pakhomov, S.; Kaszynski, P.; O'Neill, M.; Wand, M. D. *J. Mater. Chem.* **2004**, *14*, 1544–1553. Januszko, A.; Glab, K. L.; Kaszynski, P.; Patel, K.; Lewis, R. A.; Mehl, G. H.; Wand, M. D. *J. Mater. Chem.* **2006**, *16*, 3183–3192. Jasinski, M.; Jankowiak, A.; Januszko, A.; Bremer, M.; Pauluth, D.; Kaszynski, P. *Liq. Cryst.* **2008**, *35*, 343–350.
(28) Jelinek, T.; Plesek, J.; Hermanek, S.; Stibr, B. *Collect. Czech. Chem. Commun.* **1986**, *51*, 819–829.
(29) Jelinek, T.; Baldwin, P.; Scheidt, W. R.; Reed, C. A. *Inorg. Chem.* **1993**, *32*, 1982.
(30) Jelinek, T.; Plesek, J.; Mares, F.; Hermanek, S.; Stibr, B. *Polyhedron* **1987**, *6*, 1981–1986.
(31) Finze, M. *Chem.—Eur. J.* **2009**, *15*, 947–962.
(32) Ivanov, S. V.; Rockwell, J. J.; Miller, S. M.; Anderson, O. P.; Solntsev, K. A.; Strauss, S. H. *Inorg. Chem.* **1996**, *35*, 7882–7891.
(33) Brellochs, D. In *Contemporary Boron Chemistry*; Davidson, M. G., Hughes, A. K., Marder, T. B., Wade, K., Eds.; Royal Society of Chemistry: Cambridge, England, 2000, pp 212−214.
(34) Jelinek, T.; Kilner, C. A.; Thornton-Pett, M.; Kennedy, J. D. *Chem. Commun.* **2001**, 1790–1791.
(35) Franken, A.; Carr, M. J.; Clegg, W.; Kilner, C. A.; Kennedy, J. D. *Dalton Trans.* **2004**, 3552–3561.
(36) Sivaev, I. B.; Starikova, Z. A.; Petrovskii, P. V.; Bregadze, V. I.; Sjöberg, S. *J. Organomet. Chem.* **2005**, *690*, 2790–2795.
(37) Franken, A.; Kilner, C. A.; Thornton-Pett, M.; Kennedy, J. D. *Collect. Czech. Chem. Commun.* **2002**, *67*, 869–912.
(38) Ringstrand, B.; Balinski, A.; Franken, A.; Kaszynski, P. *Inorg. Chem.* **2005**, *44*, 9561–9566.
(39) Kaszynski, P.; Pakhomov, S.; Young, V. G., Jr. *Collect. Czech. Chem. Commun.* **2002**, *67*, 1061–1083.
(40) Hertler, W. R.; Knoth, W. H.; Muetterties, E. L. *J. Am. Chem. Soc.* **1964**, *86*, 5434–5439.
(41) Knoth, W. H.; Hertler, W. R.; Muetterties, E. L. *Inorg. Chem.* **1965**, *4*, 280–287.
(42) Hertler, W. R.; Knoth, W. H.; Muetterties, E. L. *Inorg. Chem.* **1965**, *4*, 288–293.
(43) Knoth, W. H. *J. Am. Chem. Soc.* **1966**, *88*, 935–939.
(44) Naoufal, D.; Grüner, B.; Bonnetot, B.; Mongeot, H. *Polyhedron* **1999**, *18*, 931–939.
(45) Kaszynski, P.; Huang, J.; Jenkins, G. S.; Bairamov, K. A.; Lipiak, D. *Mol. Cryst. Liq. Cryst.* **1995**, *260*, 315–331.
(46) Komura, M.; Nakai, H.; Shiro, M. *J. Chem. Soc., Dalton Trans.* **1987**, 1953–1956.
(47) Naoufal, D.; Bonnetot, B.; Mongeot, H.; Grüner, B. *Collect. Czech. Chem. Commun.* **1999**, *64*, 856–864.
(48) Bragin, V. I.; Sivaev, I. B.; Bregadze, V. I.; Votinova, N. A. *J. Organomet. Chem.* **2005**, *690*, 2847–2849.
(49) Knoth, W. H. *Organometallics* **1985**, *4*, 207–208.
(50) Ringstrand, B.; Kaszynski, P.; Franken, A. *Inorg. Chem.* **2009**, *48*, 7313–7329.

highly unstable,[39] and their usefulness as synthetic intermediates is limited.

Now, we report another important step in the chemistry of the {*closo*-1-CB_9} cluster, the preparation of amino acid **4** and its dinitrogen derivative **5**, which completes the development of key 1,10-heterobifunctional derivatives of the [*closo*-1-CB_9H_{10}]$^-$ cluster and opens new horizons for applications of this cluster in advanced materials and biological investigations.

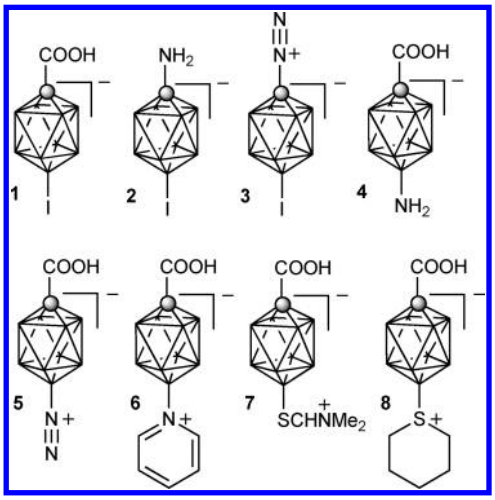

Here we describe the preparation of amino acid **4** from readily available [*closo*-1-CB_9H_8-1-COOH-10-I]$^-NMe_4^+$ (**1**[**NMe$_4$**]),[38] its diazotization, and formation of the nitrogen derivative [*closo*-1-CB_9H_8-1-COOH-10-N_2] (**5**). The latter is extensively characterized by structural, spectroscopic, thermochemical, and electrochemical methods aided by quantum-mechanical calculations. Several transformations of the dinitrogen acid **5** are demonstrated including conversion to pyridinium **6** and acid **7** containing a protected mercapto functionality. The latter was converted further to sulfonium acid **8**. Both, pyridinium acid **6** and sulfonium acid **8** were structurally characterized, and simple transformations (esterification) of the carboxyl group were demonstrated.

Results

Synthesis. [*closo*-1-CB_9H_8-1-COO-10-NH_3] (4). Amination of iodo acid **1** with ammonia equivalents was envisioned using the Buchwald-Hartwig conditions.[51] However, the reactions could not be run in toluene, a common solvent used for typical amination reactions because of the low solubility of the **1**[**NMe$_4$**] salt. Also, harsh bases such as alkali *tert*-butoxides could not be used in this process because of possible attack on the {*closo*-1-CB_9} cage. For these reasons tetrahydrofuran (THF) was the solvent of choice, and Cs_2CO_3 was the preferred base.

Our initial attempts at aminating **1** were unsuccessful. Reactions of the iodo acid **1**[**NMe$_4$**] with aqueous NH_3, according to the literature procedure,[52] or 2 equiv of diallyamine[53] with Cs_2CO_3 and 2 mol % Pd_2dba_3/8 mol %

Scheme 1

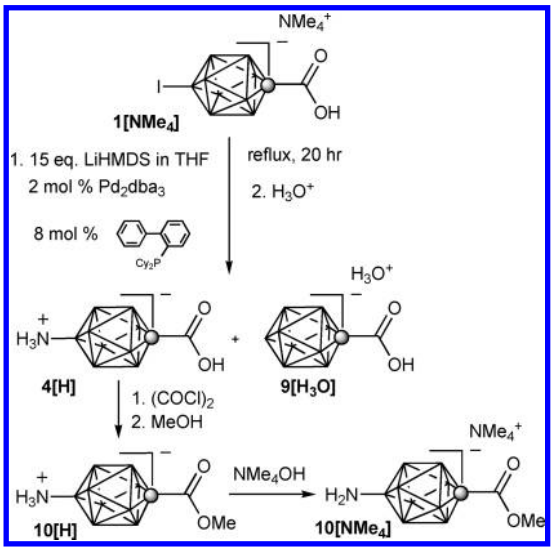

S-Phos[54] in refluxing THF showed no product formation after 24 h. Similar reactions using the latter conditions with 5 equiv of benzophenone imine,[55] or *tert*-butylcarbamate[56] were slow, taking at least 5 days to complete. Attempts to perform the amination of ethyl ester of iodo acid **1**[**NMe$_4$**] using these conditions failed, and no reaction was observed after several days.

Metal salts of hexamethyldisilazane (HMDS) as the ammonia equivalent were more promising. A reaction of **1**[**NMe$_4$**] with 5 equiv of $Zn(HMDS)_2$[57] and $[HPCy_3]^+BF_4^-$, as the phosphine ligand precursor, in THF was approximately 10% complete after 24 h at reflux. However, deiodinated product, acid [*closo*-1-CB_9H_9-1-COOH]$^-$ (**9**), was the major product observed by ^{11}B NMR. Reactions with LiHMDS[58,59] as the ammonia equivalent were more successful although deiodination of **1** was still observed. Brief optimization of the reaction conditions revealed that by increasing the amounts of LiHMDS to 15 equiv and using 2-(dicyclohexylphosphine)biphenyl as the phosphine ligand, the ratio of amino acid **4**[**H**] to parent acid **9**[**H_3O**] improved to 5:1 (Scheme 1).[60] Excess of LiHMDS beyond 15 equiv did not improve the ratio. When $[HP(t\text{-}Bu)_3]BF_4$ was used as the phosphine ligand source, the parent [*closo*-1-CB_9H_{10}]$^-$ anion was obtained as the major product apparently by deiodination at the B(10) vertex and decarboxylation at the C(1) vertex of iodo acid **1**. A summary for the results for optimization of the LiHMDS reaction is presented in the Supporting Information.

Separation of the amino acid **4**[**H**] from acid **9**[**H_3O**] was accomplished by preferential extraction of the **9**[**NEt$_4$**] ion pair with CH_2Cl_2 from an aqueous solution

(51) Abaev, V. T.; Serdyuk, O. V. *Russ. Chem. Rev.* **2008**, *77*, 177–192.
(52) Xia, N.; Taillefer, M. *Angew. Chem., Int. Ed.* **2009**, *48*, 337–339.
(53) Jaime-Figueroa, S.; Liu, Y.; Muchowski, J. M.; Putman, D. G. *Tetrahedron Lett.* **1998**, *39*, 1313–1316.
(54) Charles, M. D.; Schultz, P.; Buchwald, S. L. *Org. Lett.* **2005**, *7*, 3965–3968.
(55) Wolfe, J. P.; Ahman, J.; Sadighi, J. P.; Singer, R. A.; Buchwald, S. L. *Tetrahedron Lett.* **1997**, *38*, 6367–6370.
(56) Hartwig, J. F.; Kawatsura, M.; Hauck, S. I.; Shaughnessy, K. H.; Alcazar-Roman, L. M. *J. Org. Chem.* **1999**, *64*, 5575–5580.
(57) Lee, D.-Y.; Hartwig, J. F. *Org. Lett.* **2005**, *7*, 1169–1172.
(58) Lee, S.; Jørgensen, M.; Hartwig, J. F. *Org. Lett.* **2001**, *3*, 2729–2732.
(59) Huang, X.; Buchwald, S. L. *Org. Lett.* **2001**, *3*, 3417–3419.
(60) Amination reactions of a mixture of 6- and 10-iodo isomers [*closo*-1-CB_9H_8-1-COOH-6-I]$^-$ and [*closo*-1-CB_9H_8-1-COOH-10-I]$^-$ (**1**) under the same conditions demonstrated similar reactivity of both isomers.

Scheme 2

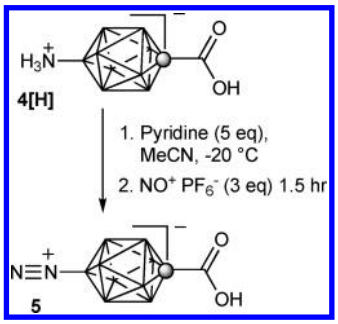

of the two products containing $Et_4N^+Br^-$. After acidification, the protonated amino acid **4[H]** was extracted to ether and isolated in purity greater than 90% (by ^{11}B NMR) and in yields ranging from 40% to 50%. The protonated form of the amino acid [*closo*-1-CB_9H_8-1-COOH-10-NH_3] (**4[H]**) was treated with 0.9 equiv of $Me_4N^+OH^-\cdot 5H_2O$ to obtain pure salt **4[NMe$_4$]** after washing with ether followed by boiling MeCN. Acidification of **4[NMe$_4$]** and extraction to ether provided a convenient method for the preparation of pure **4[H]**. The two products, **4[H]** and **9[H$_3$O]**, can also be separated by chromatography, but with lower overall yield.

[*closo*-1-CB$_9$H$_8$-1-COOH-10-N$_2$] (5). Diazotization of amino acid **4** was surprisingly difficult. Attempts to diazotize **4[H]** in aqueous AcOH, conditions used for the parent amine [*closo*-1-CB_9H_9-1-NH_3],[50] were unsuccessful and only the starting amino acid was recovered. A similar result was obtained with $NO^+PF_6^-$ as the diazotizing reagent under conditions used for weakly nucleophilic anilines.[61] When amino acid **4[H]** was allowed to react with 2.5 equiv of $NO^+PF_6^-$ overnight at room temperature instead at −20 °C, a new species with lower boron cage symmetry (according to ^{11}B NMR) and *m*/*z* of 271 (FAB-MS) was formed as the sole product. This result suggests that amino acid **4** was substituted, presumably at the B(6) vertex, which is preferred in electrophilic attack on the [*closo*-1-CB_9H_{10}]$^-$ cluster.[8,32] Attempts to further elucidate the structure were not made.

The negative results for the diazotization of **4** under typical conditions prompted us to conduct more detailed investigations. Diazotization of methyl ester of acid **4**, [*closo*-1-CB_9H_8-1-COOMe-10-NH_2]$^-$ (**10[NMe$_4$]**, Scheme 1) with $NO^+PF_6^-$ resulted in complete conversion of **10[NMe$_4$]**, and the formation of two products in 85:15 ratio with a significantly shielded B(10) nucleus. Analysis revealed that the major product was the protonated amino ester **10[H]**, while the minor product with a more shielded B(10) nucleus ($\Delta\delta$ = −26.7 ppm) was the expected dinitrogen ester **11**. The complete and clean transformation of ester **10[NMe$_4$]** to **11** was accomplished by addition of pyridine to the reaction mixture. A similar approach was taken for diazotization of acid **4[H]**. Initially, the reaction was conducted in neat pyridine, but brief optimization[62] led to MeCN containing 5.0 equiv of pyridine as the appropriate medium for the reaction.

(61) Lipilin, D. L.; Belyakov, P. A.; Strelenko, Y. A.; Churakov, A. M.; Smirnov, O. Y.; Ioffe, S. L.; Tartakovsky, V. A. *Eur. J. Org. Chem.* **2002**, 3821–3826.

(62) For details see Supporting Information.

Scheme 3

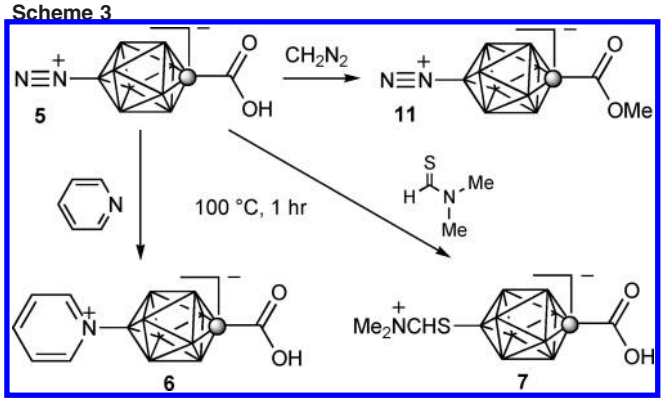

Scheme 4

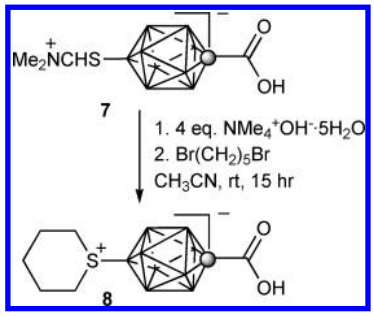

The yield of isolated dinitrogen acid [*closo*-1-CB_9H_8-1-COOH-10-N_2] (**5**) was about 80% after chromatographic separation (Scheme 2). Diazotization of crude **4[H]** gave a lower yield of about 60%. In none of the diazotization reactions in the presence of pyridine was the formation of **6** observed (vide infra).

Other bases such as NaH or solid K_2CO_3 were less effective, and incomplete conversion was observed even with large excess of $NO^+PF_6^-$.

Reactivity of [*closo*-1-CB$_9$H$_8$-1-COOH-10-N$_2$] (5). Reactions of dinitrogen acid **5** in neat pyridine and *N*,*N*-dimethylthioformamide gave pyridinium acid **6** and masked mercapto acid **7**, respectively, as the sole products (Scheme 3). Masked mercaptan **7** was isolated as a crude product and used without further purification, whereas pyridinium **6** was isolated in 90% yield after chromatographic separation. In contrast to [*closo*-1-CB_9H_9-1-N_2],[50] reaction of dinitrogen **5** required heating to about 100 °C, which is typical for reactions of *B*−dinitrogen derivatives of [*closo*-$B_{10}H_{10}$]$^{2-}$.[40−49]

The acid **5** also reacted smoothly with diazomethane to give methyl ester **11** in 78% yield (Scheme 3). This provides an alternative to the formation of **11** by diazotization of amino ester **10**.

The synthetic utility of the protected mercaptan **7** was demonstrated by formation of sulfonium derivative **8** under hydrolytic conditions in the presence of a base and 1,5-dibromopentane. The optimized reaction required 4 equiv of base ($Me_4N^+OH^-$), and the product **8** was isolated by chromatographic methods in 60% yield (Scheme 4). With fewer equivalents of base, the *S*-alkylation competed with alkylation of the carboxyl group.

Finally, chemical transformations of the carboxyl group in the presence of the onium fragments in acids **6** and **8** were demonstrated. Thus, using 2-chloro-3,

Scheme 5

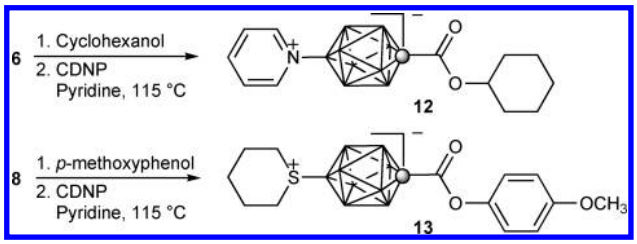

5-dinitropyridine (CDNP) as a condensation agent,[63] zwitterion **6** was converted to an ester of a secondary alcohol (**12**), and acid **8** gave an ester of a phenol (**13**) in 75% and 54% yields, respectively (Scheme 5). Identical reactions with DCC were less clean and efficient.

Reaction with PhCN and Kinetic Data for [*closo*-1-CB$_9$H$_8$-1-COOMe-10-N$_2$] (11). Decomposition of dinitrogen ester **11** in dry PhCN at elevated temperatures (> 100 °C) gave a single product identified as zwitterion **14**. Upon addition of moist PhCN to the reaction mixture, the zwitterion **14** was converted quantitatively to benzamide **15** (Scheme 6), which was isolated and partially characterized. An attempt to thermolyze **11** in MeCN was unsuccessful, and no trace of product was observed after 1 h at 80 °C. The clean transformation of **11** in PhCN to a single product permitted kinetics analysis of this reaction, which is believed to involve the heterolytic cleavage of the B−N bond as the rate-determining step.

Thus, kinetics of decomposition of **11** in dry PhCN was followed by ^{11}B NMR spectroscopy in a temperature range of 125 °C−140 °C.[62] Intensities of the disappearing B(10) signal at 19.8 ppm and the growing peak at 29.1 ppm were used to calculate the ratio of **11** to **14**. Standard kinetic analysis using the Eyring equation found $\Delta H^{\ddagger} = 33.9 \pm 1.4$ kcal mol^{-1}, $\Delta S^{\ddagger} = 10.0 \pm 3.5$ cal mol^{-1} K^{-1}, and $\Delta G^{\ddagger}_{298} = 30.9 \pm 1.4$ kcal mol^{-1}.

Similar studies with the carboxylate anion of **5** could not be performed because of the insolubility of salt **5**$^-$[**NMe$_4$**] in PhCN, even at 140 °C.

Molecular and Crystal Structures. Colorless crystals of **5**, **6**, and **8** were grown by slow evaporation of a CH_2Cl_2 solution containing a few drops of MeOH. Solid-state structures for all three compounds were determined by X-ray diffraction (Figure 2),[64] and selected bond lengths and angles are shown in Table 1.

All three acids form dimeric structures in the solid state. In the crystal of dinitrogen acid **5**, the two monomers are related by an inversion center. In contrast, the dimeric pair in the solid structure of **8** is unsymmetric, and both monomeric acids are unique molecules, while in the crystal of pyridinium acid **6**, there are four unique molecules (two unsymmetric unique dimers).

Scheme 6

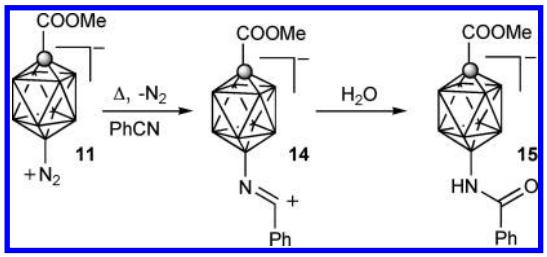

The carboxyl group in each acid adopts a pseudo-staggered conformation relative to the {*closo*-1-CB$_9$} cage. The deviation of the COOH group from the ideal staggered orientation varies from as little as 5°, observed in the solid-state structure of **5** and one of the molecules of **6**, to 18° in acid **8** and 20° in two molecules of pyridinium acid **6**. The pair of carboxyl groups are ideally co-planar in **5**, nearly co-planar in pyridinium acid **6** (the interplanar angle of about 8°), and significantly off co-planarity in sulfonium acid **8** (the interplanar angle of 20°).

The B−N bond length of 1.4981(17) Å observed in **5** is similar to 1.489(6) Å and 1.499(2) Å reported for [*closo*-B$_{10}$H$_9$-1-N$_2$]$^-$[65] and [*closo*-B$_{10}$H$_8$-1,10-(N$_2$)$_2$],[66] respectively. Also the observed N−N distance in **5** (1.0905(15) Å) is close to those reported for the {*closo*-B$_{10}$} analogues (1.097(6) Å and 1.091(2) Å).

The pyridine ring in **6** adopts a nearly ideal staggered orientation relative to the {*closo*-1-CB$_9$} cage in one dimer (2° and 4° off the ideal conformation), while in the other pair the deviation is larger (18° and 20°). As a result, the interplanar angle between the COOH and C$_5$H$_5$N groups, measured using the first three atoms from the cage, deviates about 15° from the ideal 45° (see Figure 3) in each molecule. The overall interplanar angle between the pyridinium rings in the two unique dimers is 1.5° and 6.4°.

The orientation of the thiacyclohexane ring in acid **8** is 15° in one monomer and 30° in another monomer away from the ideal staggered conformation in which the sulfur lone pair eclipses the B−B bond (Figure 3). The staggered conformation has been found to be the conformation minimum in theoretical models (vide infra) and observed in solid-state structures of related sulfonium derivatives of [*closo*-B$_{10}$H$_{10}$]$^{2-}$.[67,68] For instance, in the structure of [*closo*-B$_{10}$H$_8$-1,10-(SMe$_2$)$_2$] the two SMe$_2$ groups are about 2° and 16° away from the ideal staggered conformation, and the B−S bond length (1.866(3) Å) is similar to that observed in **8**.[67]

Analysis of the {*closo*-1-CB$_9$} cage geometry indicates that the pyramidalization of the B(10) apex is greater for more electronegative onium substituents. The X−B(10) distance is smaller and consequently the B(10)···C(1)

(63) Takimoto, S.; Abe, N.; Kodera, Y.; Ohta, H. *Bull. Chem. Soc. Jpn.* **1983**, *56*, 639–640.

(64) Crystal data for **5** (CCDC no. 744000): $C_2H_9B_9N_2O_2$ monoclinic, $P2_1/n$, $a = 7.022(2)$ Å, $b = 11.389(4)$ Å, $c = 12.815(4)$ Å, $\beta = 96.212(5)°$; $V = 1018.8(6)$ Å^3, $Z = 4$, $T = 173(2)$ K, $\lambda = 0.71073$ Å, $R(F^2) = 0.0384$ or $R_w(F^2) = 0.1006$ (for 1945 reflections with $I > 2\sigma(I)$). Crystal data for **6** (CCDC no. 743999): $C_7H_{14}B_9NO_2$, monoclinic, $P2_1/n$, $a = 14.275(4)$ Å, $b = 12.184(3)$ Å, $c = 30.538(8)$ Å, $\beta = 95.377(4)°$; $V = 5288(3)$ Å^3, $Z = 16$, $T = 173(2)$ K, $\lambda = 0.71073$ Å, $R(F^2) = 0.0541$ or $R_w(F^2) = 0.1358$ (for 7029 reflections with $I > 2\sigma(I)$). Crystal data for **8** (CCDC no. 744001): $C_7H_{19}B_9O_2S$, monoclinic, $P2_1/c$, $a = 15.988(5)$ Å, $b = 19.377(6)$ Å, $c = 9.655(3)$ Å, $\beta = 98.348(5)°$; $V = 2959.4(16)$ Å^3, $Z = 8$, $T = 173(2)$ K, $\lambda = 0.71073$ Å, $R(F^2) = 0.0428$ or $R_w(F^2) = 0.0979$ (for 4900 reflections with $I > 2\sigma(I)$). For details see Supporting Information.

(65) Ng, L.-L.; Ng, B. K.; Shelly, K.; Knobler, C. B.; Hawthorne, M. F. *Inorg. Chem.* **1991**, *30*, 4278–4280.

(66) Whelan, T.; Brint, P.; Spalding, T. R.; McDonald, W. S.; Lloyd, D. R. *J. Chem. Soc., Dalton Trans.* **1982**, 2469–2473.

(67) Hall, H. D.; Ulrich, B. D.; Kultyshev, R. G.; Liu, J.; Liu, S.; Meyers, E. A.; Gréau, S.; Shore, S. G. *Collect. Czech. Chem. Commun.* **2002**, *67*, 1007–1024.

(68) Schramm, K. D.; Ibers, J. A. *Inorg. Chem.* **1977**, *16*, 3287–3293.

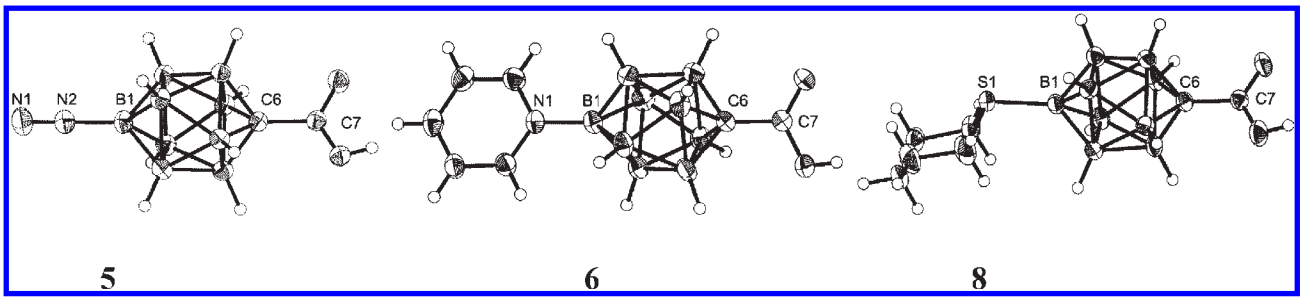

Figure 2. Thermal ellipsoid diagram representations of selected molecules of [*closo*-1-CB_9H_8-1-COOH-10-N_2] (**5**), [*closo*-1-CB_9H_8-1-COOH-10-C_5H_5N] (**6**), and [*closo*-1-CB_9H_8-1-COOH-10-$C_5H_{10}S$] (**8**), and drawn at 50% probability. Selected interatomic distances and angles for **5**, **6**, and **8** are listed in Table 1.

Table 1. Selected Experimental and Calculated Bond Lengths and Angles for [*closo*-1-CB_9H_8-1-COOH-10-N_2] (**5**), [*closo*-1-CB_9H_8-1-COOH-10-C_5H_5N] (**6**), and [*closo*-1-CB_9H_8-1-COOH-10-$C_5H_{10}S$] (**8**)

	5		**6**		**8**	
	exp.[a]	calcd.[b]	exp.[a]	calcd.[b]	exp.[a]	calcd.[b]
			Distances/Å			
B(10)−X[c]	1.4981(17)[d,e]	1.461[d]	1.525[d]	1.520[d]	1.858[f]	1.854[f]
B(10)-B[c]	1.6702	1.674	1.676	1.676	1.680	1.676
C_{cage}−B[c]	1.6053	1.602	1.601	1.603	1.607	1.604
C_{cage}−C_{COOH}[c]	1.4859(16)	1.489	1.482	1.484	1.485	1.485
C(1)···B(10)[c]	3.429	3.436	3.471	3.465	3.478	3.463
			Angles/deg			
X−B−B[c]	127.3[d]	127.6[d]	128.7[d]	128.5[d]	128.6[f]	128.4[f]
C_{COOH}-C_{cage}-B[c]	125.0	125.1	125.4	125.3	125.4	125.3

[a] See ref 64. [b] MP2/6-31G(d,p) level geometry optimization at C_s (**5** and **8**) or C_1 (**6**) point group symmetry for monomeric acids. [c] Average value for all equivalent bonds or angles in all unique molecules. Numbering system according to the chemical structure. [d] X = N. [e] The N−N distance: experimental 1.0905(15) Å and calculated 1.138 Å. [f] X = S.

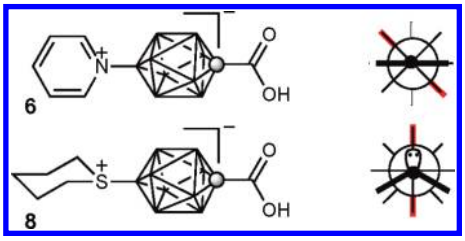

Figure 3. Extended Newman projection along the long molecular axes of **6** and **8** showing the staggered (minimum) conformations. The bars represent the substituents, and the filled circle is the nitrogen or sulfur atom.

separation is markedly shorter in **5** with the most electronegative substituent N_2^+ (σ_p = 1.91)[69] than in the sulfonium **8** (SMe_2^+ σ_p = 0.90)[69] and pyridinium analogues (Table 1). Similar observations were found for derivatives of $C_2B_{10}H_{12}$.[39,70]

Computational Analysis. To shed more light on properties of **5** and its reactions with nucleophiles, we conducted quantum-mechanical calculations initially at the B3LYP/6-31G(d,p) level of theory to establish conformational minima and to obtain thermodynamic corrections. The resulting structures were used as starting points to optimize geometry and calculate the self-consistent field (SCF) energies at the MP2/6-31G(d,p) level of theory. For comparison purpose, properties of the anion $\mathbf{5}^-$, the parent [*closo*-1-CB_9H_9-10-N_2] (**16**), and its isomer [*closo*-1-CB_9H_9-1-N_2] (**17**)[50] were also considered at the same level of theory. Computational results are shown in Figure 4, Tables 2 and 3, and equilibrium geometries are provided in the Supporting Information.

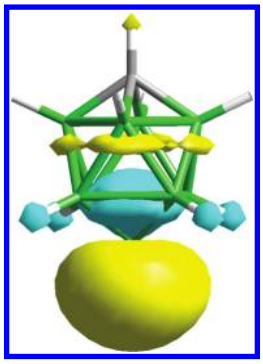

Figure 4. MP2/6-31G(d,p) derived contour for the LUMO (E = 0.21 eV) of ylide **19**. Nearly identical contours are found for **18** and $\mathbf{18}^-$.

Initially, the performance of the adopted computational protocol was tested on acids **5**, **6**, and **8**, whose solid-state structures were established experimentally. Both DFT and MP2 methods well reproduced the experimentally observed conformational minima of the substituents in the three compounds (Figure 3). Detailed comparison of the theoretical and experimental bond lengths demonstrated that the MP2-level geometry optimizations performed better with the mean difference of 0.0001 ± 0.006 Å (absolute mean 0.005 ± 0.004 Å) than the DFT method (mean error = −0.006 ± 0.008 Å, absolute mean error 0.007 ± 0.007 Å).[71] Selected results for the MP2/6-31G(d,p) calculations are shown in Table 1.

Formation, Structure, and Reactivity of the Boronium Ylides. Experimental results indicate that reactions of **5** involve boronium ylide **18**. Calculations demonstrated that its formation by heterolytic cleavage of the B−N bond in **5** is endothermic by 41.8 kcal/mol (Table 2) and practically identical to that calculated for ester [*closo*-1-CB_9H_8-1-COOMe-10-N_2] (**11**). This enthalpy change is nearly the same as the formation of the parent B(10) boronium ylide **19** from [*closo*-1-CB_9H_9-10-N_2] (**16**), and

(69) Hansch, C.; Leo, A.; Taft, R. W. *Chem. Rev.* **1991**, *91*, 165–195.
(70) Hnyk, D.; Holub, J.; Hofmann, M.; Schleyer, P. v. R.; Robertson, H. E.; Rankin, D. W. H. *J. Chem. Soc., Dalton Trans.* **2000**, 4617–4622.

(71) Statistical analysis for a total of 90 bond lengths in acids **5**, **6**, and **8** excluding the C−O and N−N distances.

Table 2. Calculated Reaction Energies for Selected Dinitrogen Derivatives of the {*closo*-1-CB_9} in Gas Phase[a]

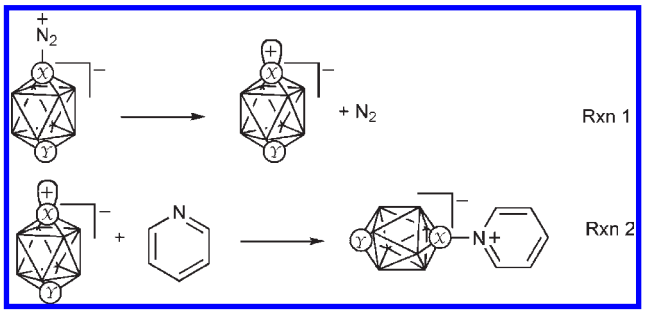

compound			*Rxn* 1			*Rxn* 2			*Rxns* 1 + 2	
	X	Y		ΔH /kcal mol^{-1}	ΔG_{298} /kcal mol^{-1}		ΔH /kcal mol^{-1}	ΔG_{298} /kcal mol^{-1}	ΔH /kcal mol^{-1}	ΔG_{298} /kcal mol^{-1}
5	B	CCOOH	**18**	41.8	31.1	**6**	−88.6	−76.2	−46.8	−45.1
5$^-$	B	CCOO-	**18**$^-$	37.0	26.2	**6**$^-$	−70.5	−57.9	−33.5	−31.7
16	B	CH	**19**	41.1	30.3	**21**	−86.8	−74.6	−45.7	−44.3
17	C	BH	**20**	33.3	20.3	**22**	−92.5	−77.7	−59.2	−57.4

[a] MP2/6-31G(d,p) level with DFT thermodynamic corrections.

Table 3. Calculated Structural Parameters for Selected Ylides[a]

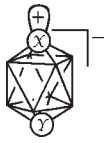

	X = B	X = B	X = B	X = C
	Y = CCOOH	Y = CCOO$^-$	Y = CH	Y = BH
	18	**18**$^-$	**19**	**20**
Geometry				
C(1)−B /Å	1.598 [b]	1.591	1.594	1.532
B(2)−B(3) /Å	1.872 1.855	1.848 1.840	1.861	1.928
B(2)−B(6) /Å	1.810 [b]	1.820 [b]	1.812	1.829
B(6)−B(7) /Å	1.931 [b]	1.916	1.928	1.894
B(10)-B_{avrg} /Å	1.628 [b]	1.624 1.630	1.628	1.678
B−C−B_{avrg} /°	111.0	110.0	111.3	125.8
B−B(10)−B_{avrg} /°	114.0 113.7	113.0 112.4	113.8	105.9
Natural Atomic Charge[c]				
C(1)	−0.74	−0.72	−0.79	−0.34
B(2)	0.08	0.07	0.05	0.07
B(6)	−0.20	−0.21	−0.21	−0.11
B(10)	0.45	0.34	0.44	−0.32
Bonding[c]				
X exo	$sp^{18.4}$ (0.18)	$sp^{29.7}$ (0.25)	$sp^{18.8}$ (0.18)	sp^{100} (0.64)
LUMO /eV	−0.03	3.21	0.21	−1.57

[a] Optimized at the MP2/6-31G(d,p) level of theory at the C_s (**18**), C_{2v} (**18**$^-$), or C_{4v} (**19** and **20**) point group symmetry. [b] Average value. [c] NBO analysis.

significantly larger, by about 8 kcal/mol, than the formation of the carbonium ylide **20** from [*closo*-1-CB_9H_9-1-N_2] (**17**).[50] Interestingly, the heterolysis of the carboxylate anion **5**$^-$ is easier by nearly 5 kcal/mol than that of the protonated form, acid **5**. The computational results are consistent with experimental data for dinitrogen derivatives **11** (vide supra) and **17**.[50] The calculated larger change of free energy, $\Delta\Delta G_{298}$ = 10.8 kcal/mol, in the formation of ylide **18** as compared to **20** in gas phase corresponds to the observed higher activation energy $\Delta\Delta G^{\ddagger}_{298}$ = 5.8 kcal/mol for the thermolysis of **11** relative to **17** in a dielectric medium.

The reactivity of the ylides was assessed from their reactions with pyridine. The results show that trapping of ylides **18**, **19**, and **20** by pyridine and the formation of the corresponding adducts **6**, **21**, and **22**[50] is highly exothermic (about 90 kcal/mol), and the order of the thermal effect follows **20** > **18** > **19** (Table 2). The exotherm for the reaction of the carbonium ylide **20** with pyridine is greater than that for its isomeric boronium ylide **19** by 5.7 kcal/mol. Deprotonation of ylide **18** has a significant effect on its reactivity, and trapping of carboxylate boronium ylide **18**$^-$ with pyridine has a nearly 18 kcal/mol lower exotherm relative to that of **18**.

The large exotherm for the second reaction (Table 2) overcompensates the endotherm for the ylide generation, and the overall process of transforming dinitrogen derivatives to their pyridine products is exothermic (Table 2). The relatively low energy of formation of carbonium ylide **20** and its high reactivity results in a larger overall enthalpy change for the transformation of [*closo*-1-CB_9H_9-1-N_2] (**17**) than for the B(10) analogues **5** and **16** by about 13 kcal/mol. Transformation of the deprotonated acid **5**, the anion **5**$^-$, has the lowest overall exotherm, which is lower by 13.5 kcal/mol than that for the acid **5**.

The observed reactivity of the ylides is related to their electronic structures. Both types of ylides, the boronium and carbonium, have the lowest unoccupied molecular orbital (LUMO) localized mainly on the exocyclic orbital of the electron deficient atom with some density on the non-adjacent boron atom belt. This contribution of the boron belt is more pronounced for the carbonium ylide **20** than for the boronium analogue (Figure 4). NBO analysis of the MP2 wave function demonstrates that the B(10) atom in the boronium ylides is electropositive, while the C(1) atom in carbonium ylide **20** is electronegative.

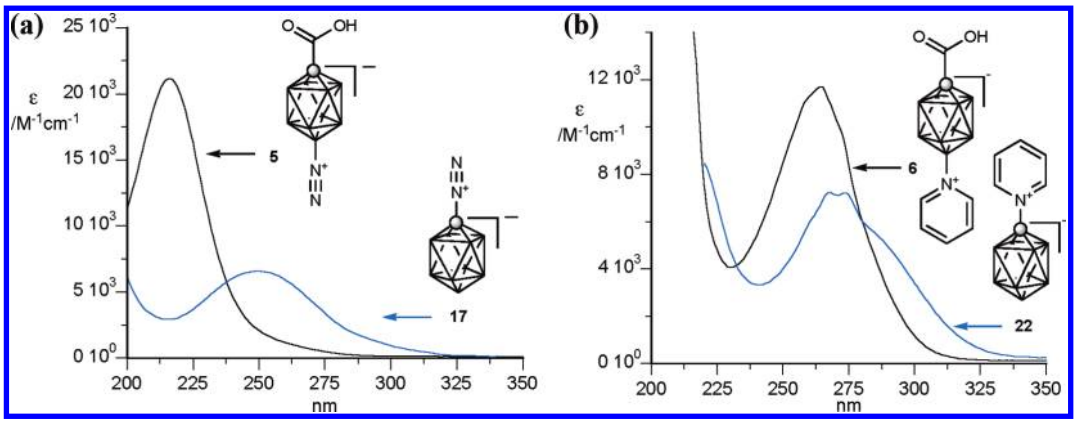

Figure 5. Electronic absorption spectra for (a) dinitrogen acid **5** and [*closo*-1-CB_9H_9-1-N_2] (**17**), and (b) pyridinium acid **6** and [*closo*-1-CB_9H_9-1-NC_5H_5] (**22**) recorded in CH_3CN.

The two types of ylides also display a difference in hybridization of the exocage orbital: the carbonium ylide has a practically pure p character, while a small fraction of an s orbital is mixed into the p orbital in the boronium ylides.

Deprotonation of the COOH group in **18** and the formation of the carboxylate ylide **18**$^-$ has a large effect on the boronium center: it increases the electron density on the exocage hybrid by nearly 40%, which consequently increases the p content of the hybrid and the energy of the LUMO by nearly 3.5 eV. These results, the charge density and the LUMO energy, are consistent with the reactivity of the ylides toward pyridine: the lower the energy of the LUMO the higher the exotherm of the reaction (Table 2).

Electronic Absorption Spectroscopy. Electronic interactions between onium substituents and the {*closo*-1-CB_9} cluster were probed using electronic absorption spectroscopy. The UV spectra of dinitrogen acid **5** and pyridinium acid **6** show strong absorption bands at 216 and 263 nm, respectively (Figure 5). The observed absorption bands are blue-shifted and have higher intensity relative to similar derivatives with the onium substituent at the C(1) vertex: [*closo*-1-CB_9H_9-1-N_2] (**17**)[50] and [*closo*-1-CB_9H_9-1-NC_5H_5] (**22**).[50] A particularly strong shift of 34 nm is observed for the pair **5** and **17**.

ZINDO//MP2/6-31G(d,p) level calculations revealed that both isomeric dinitrogen derivatives **16** and **17** exhibit similar two main $\pi \rightarrow \pi^*$ transitions. For [*closo*-1-CB_9H_9-10-N_2] (**16**), both transitions involve a combination of two excitations: from the double degenerate highest occupied molecular orbital (HOMO), with the density localized mostly on the {1-*closo*-CB_9} cage, to the double degenerate LUMO, which is localized on the N_2 fragment, and the intracage HOMO→LUMO+2 excitation. In MeCN dielectric medium, energy for both transitions shifts and for the C(1) isomer **17** merge into one absorption band at 249 nm (exp.[50] 250 nm). In contrast, the two transitions for the B(10) isomer **16** constitute separate absorption bands at 223 (f = 0.56) and 232 nm (f = 0.67). Similar calculations for the dinitrogen acid **5** showed a significantly larger number of transitions in the 220−250 nm region mainly because of the lower molecular symmetry (C_s vs C_{4v}) and the involvement of the COOH group. Nevertheless, the main transitions in **5** are essentially the same, $\pi_{cage} \rightarrow \pi_{cage}^*$ and $\pi_{cage} \rightarrow \pi_{N2}^*$, as those observed for **16** and involve orbitals shown in Figure 6. In MeCN dielectric medium, the two main

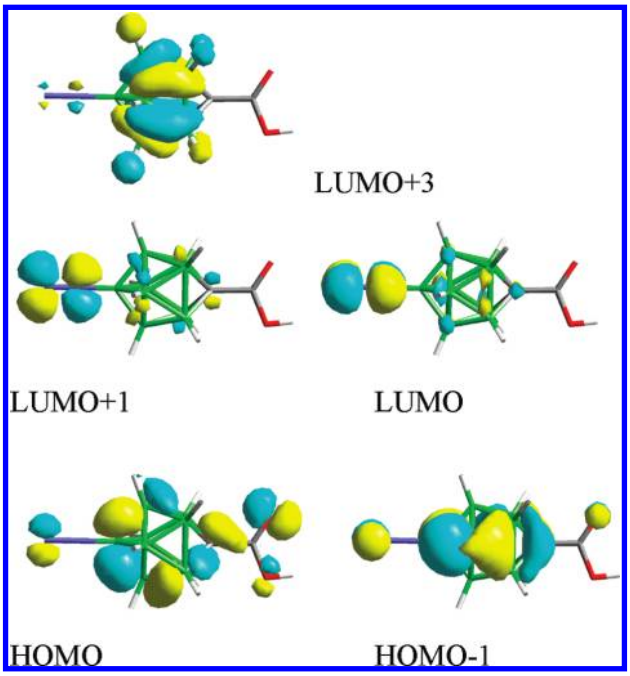

Figure 6. ZINDO-generated MO contours for **5**.

transitions for **5** are calculated at 226 (f = 0.50) and 236 nm (f = 0.54), which may appear as one broad absorption band in the UV spectrum. The experimental absorption band in **5** (Figure 5) is 15 nm blue-shifted relative the average position of the calculated bands.

The calculated blue shift of about 20 nm for the absorption band in **16** relative to **17** is consistent with a 34 nm shift observed for the pair of **5** and **17** (Figure 5a). Analysis of the MP2 wave functions for **16** and **17** demonstrated a wider HOMO−LUMO gap (~1.1 eV) in the B(10) (former) than in the C(1) (latter) isomer, due mainly to an increase of the energy of the LUMO (+0.68 eV). This can be rationalized by lower electronegativity of the B(10) than the C(1) atom and consequently higher electron density on the N_2 fragment.

Dissociation Constants Measurements. The apparent dissociation constant pK for the amino acid **4[NMe$_4$]** was measured by potentiometric titration in 50% aq. EtOH (v/v). For comparison purposes, the apparent pK values for the parent acid [*closo*-1-CB_9H_9-1-COOH]$^-$ (**9**) and benzoic acid were also measured in the same solvent.

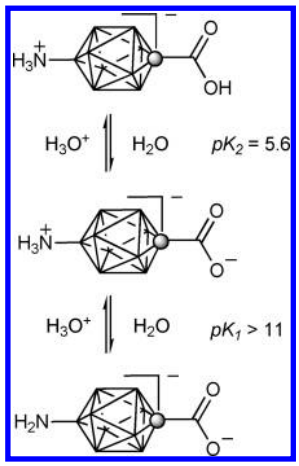

Figure 7. Apparent ionization constants pK for **4** in 50% EtOH (v/v) at 24 °C.

The results in Figure 7 for titrations of **4**[**NMe$_4$**] with acid show that the apparent pK_2 value for dissociation of the COOH in [*closo*-1-CB_9H_8-1-COOH-10-NH_3] (**4**[**H**]) is 5.61 ± 0.08, which is similar to that measured for benzoic acid in the same solvent (pK = 5.51, lit.[72] pK = 5.67, lit.[73] pK = 5.80). Titration of **4**[**NMe$_4$**] with a base gave only the lower limit (pK_1 > 11) for the apparent dissociation constant of the NH_3^+ group. A comparison of the pK_2 value for **4** with that for the parent acid [*closo*-1-CB_9H_9-1-COOH]$^-$ (**9**[**NEt$_4$**], pK = 6.36) shows that the presence of the NH_3^+ group in the antipodal B(10) position of **4**[**H**] shifts the pK value by about −0.8. The solution of the amino acid salt **4**[**NMe$_4$**] is slightly basic in 50% EtOH with a pH of about 8.6.

Discussion

The reactions reported here demonstrate the strong effect of the antipodal substituent and the impact of the negatively charged cage upon reactivity. For instance, the amination reaction of iodo acid **1** and the formation of amino acid **4** represents a rare example of *B*-amination[74] and the first example of Pd-catalyzed amination of a boron cluster with an ammonia equivalent. The reactivity of the iodine at the B(10) position appears to be highly sensitive to the substituent at the C(1) vertex; it is inactive in the presence of an alkoxycarbonyl substituent but undergoes substitution when the carboxylate group is present in the antipodal position. This result is consistent with our previous observations of Pd-catalyzed Negishi-type alkylation of the iodo acid **1** and its ester.[8] Both results suggest that the moderately electron withdrawing alkoxycarbonyl substituent (σ_p = 0.45)[69] at C(1) completely deactivates the B(10)−I bond toward oxidative addition of Pd(0) or shuts down the transmetalation step in the catalytic cycle. On the other hand, the carboxylate group (σ_p = 0.00)[69] at the C(1) position allows for the reaction to proceed to completion.

The two substituents, COOR and COO^-, have similar effect on reactivity of dinitrogen derivatives **5** and **5**$^-$. However, analysis of computational results indicates that deprotonation of the COOH group in **5** and the formation of the carboxylate anion COO^- in **5**$^-$ has a more pronounced effect on the reactivity than can be expected on the basis of Hammett σ parameters.[69] It appears that the ionization of the COOH group injects significant electron density into the {*closo*-1-CB_9} cage and to the B(10) position in particular. This is evident from the calculated higher reactivity of the anion **5**$^-$, and also higher charge density at the B(10) position and lower electrophilicity of the boronium ylide **18**$^-$, as compared to the analogous carboxylic acid derivatives (**5** and **18**) and the parent boronium ylide **19** (Tables 2 and 3). These results indicate that the relative impact of the antipodal substituents on reactivity of the {*closo*-1-CB_9} derivatives follows: COOH ~ COOR ~H > COO^-, which is different than the order of the Hammett parameter values σ_p (COOH ~ COOR > COO^- ~ H).[69]

The amino group in **4** is unusually basic. The measured pK for the conjugate acid appears to be higher than that reported for quinuclidinium in the same solvent (pK = 10.2).[75] A consequence of this basicity is the facile protonation of the NH_2 group and the formation of the zwitterion [*closo*-1-CB_9H_8-10-NH_3-1-COOH] (**4**[**H**]). The zwitterionic structure is consistent with ^{11}B NMR spectra for **4**[**H**] and its derivatives. The B(10) nucleus has nearly the same chemical shift in **4**[**H**] and its methyl ester **10**[**H**] (37.0 and 37.1 ppm, respectively). Treatment of the ester with 1 equiv of NMe_4OH leads to deshielding of the B(10) nucleus by nearly 10 ppm, which is consistent with the presence of the NH_2 group in **10**[**NMe$_4$**]. On the other hand, neutralization of **4**[**H**] with 1 equiv of NMe_4OH results in 3.4 ppm shielding of the B(10) nucleus in CD_3OD solvent. Since the B(10) nucleus is shielded by 5.9 ppm after deprotonation of dinitrogen acid **5** and formation of **5**$^-$[**NMe$_4$**] in CD_3CN, the structure of **4**[**NMe$_4$**] is consistent with the zwitterion [*closo*-1-CB_9H_8-1-COO-10-NH_3]$^-$. Interestingly, addition of another equivalent of NMe_4OH to the solution of **4**[**NMe$_4$**] does not affect the chemical shift of the B(10) nucleus, which may suggest that the pK for the NH_3^+ group is >15 in CD_3OD.[76]

The high basicity of the amino group in **4** is also evident from its chemical reactivity: upon protonation in **4**[**H**] it becomes completely inert toward electrophiles such as acid chlorides and NO^+. Thus, the zwitterion **4**[**H**] can be converted to methyl ester **10** in high yield apparently through the acid chloride [*closo*-1-CB_9H_8-1-COCl-10-NH_3] (Scheme 1). Also, the total resistance of **4**[**H**] to diazotization in aqueous medium is in sharp contrast to the same reaction of *p*-aminobenzoic acid.[77] The high basicity of the amino group and consequently tight N−H bond in the ammonio group is also evident from the observed $^1J_{N-H}$ = 34 and 42 Hz found for **4**[**H**] and **10**[**H**] in CD_3CN solutions, respectively.[78]

The high basicity observed for the amino group in **4** is consistent with reports for other amino-*closo*-borates and our calculations. For instance, the amines [*closo*-$B_{10}H_9$-1-NH_2]$^{2-}$ and [*closo*-$B_{12}H_{11}NH_2$]$^{2-}$ are highly basic and "the *N*-protonated forms of these amino compounds could

(72) Niazi, M. S. K.; Mollin, J. *Bull. Chem. Soc. Jpn.* **1987**, *60*, 2605–2610.
(73) Wilcox, C. F., Jr.; McIntyre, J. S. *J. Org. Chem.* **1965**, *30*, 777–780.
(74) Mukhin, S. N.; Kabytaev, K. Z.; Zhigareva, G. G.; Glukhov, I. V.; Starikova, Z. A.; Bregadze, V. I.; Beletskaya, I. P. *Organometallics* **2008**, *27*, 5937–5942.
(75) Hoefnagel, A. J.; Hoefnagel, M. A.; Wepster, B. M. *J. Org. Chem.* **1981**, *46*, 4209–4211.
(76) pK values measured in MeOH are higher than those in 50% EtOH. For PhCOOH the difference is 0.86; Bright, W. L.; Briscoe, H. T. *J. Phys. Chem.* **1933**, *37*, 787–796.
(77) For example :Morita, Y.; Agawa, T. *J. Org. Chem.* **1992**, *57*, 3658–3662. McNab, H.; Monahan, L. C. *J. Chem. Soc. Perkin Trans. 1* **1989**, 419–424.
(78) A $^1J_{N-H}$ = 46 Hz for a partially collapsed triplet was reported for anhydrous NH_3: Ogg, R. A., Jr.; Ray, J. D. *J. Chem. Phys.* **1957**, *26*, 1515–1516.

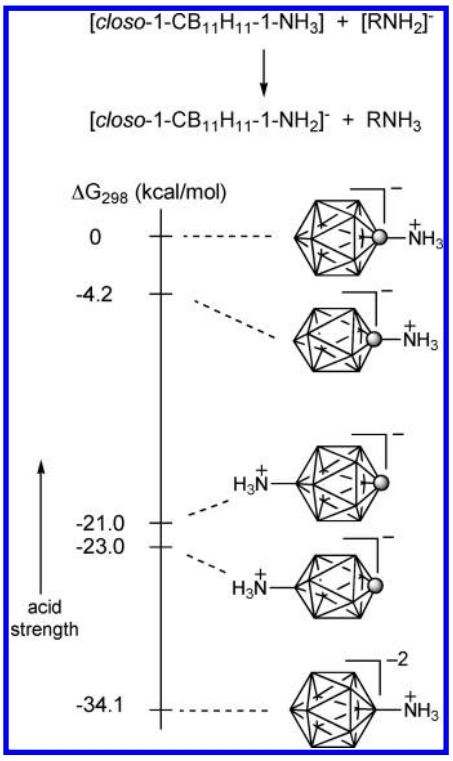

Figure 8. Free energy change for the acid−base reaction shown on the top obtained at the MP2/6-31+G(d,p)//MP2/6-31G(d,p) level of theory with DFT thermodynamic corrections in 50% EtOH dielectric medium (ε = 52.5).

be isolated directly from alkaline solutions."[79] A similar observation was made for $[closo\text{-}B_{12}H_{11}NHMe_2]^-$ which "is such a weak acid that OH^- does not remove the proton from the quaternary nitrogen".[80] It was also reported that $[closo\text{-}B_{10}H_8\text{-}1,10\text{-}(NH_2)_2]^{2-}$ could not be diazotized in aqueous medium "possibly because the concentration of these anions in aqueous acid solution is negligible".[43,81] A comparison of experimental data for $[closo\text{-}1\text{-}CB_{11}H_{11}\text{-}1\text{-}NH_3]$ (pK_a = 6.0 in 50% EtOH[28] or H_2O[31]) and $[closo\text{-}1\text{-}CB_{11}H_{11}\text{-}2\text{-}NH_3]$ indicates that the *B*−ammono derivative is significantly less acidic than the former isomer by more that 5.5 units.[31] These experimental results are supported by computational data which show a difference in pK_a for the two amines of about 7 units, and estimate the pK_a value for $[closo\text{-}B_{12}H_{11}NH_3]^-$ at about 20![31] Our calculations shown in Figure 8 also demonstrate that the *B*−amino *closo*-borates are significantly more basic than the *C*−amino isomers, and that the amine basicity follows the order $\{closo\text{-}B_{12}\} > \{closo\text{-}1\text{-}CB_9\} > \{closo\text{-}CB_{11}\}$. These findings are consistent with the observed difference in reactivity of $[closo\text{-}1\text{-}CB_9H_9\text{-}1\text{-}NH_3]$, which can be diazotized under aqueous acidic conditions,[50] and the $[closo\text{-}1\text{-}CB_9H_8\text{-}1\text{-}COOH\text{-}10\text{-}NH_3]$ (**4**[**H**]), which requires a stronger base for a successful diazotization. To our knowledge, the preparation of **5** is the first example of diazotization under homogeneous basic conditions.[82]

(79) Hertler, W. R.; Raasch, M. S. *J. Am. Chem. Soc.* **1964**, *86*, 3661–3668.
(80) Knoth, W. H.; Miller, H. C.; England, D. C.; Parshall, G. W.; Muetterties, E. L. *J. Am. Chem. Soc.* **1962**, *84*, 1056–1057.
(81) The author in ref 43 quotes a preliminary $[pK_a]_{(MeCN)}$ value of 12.2 for $[closo\text{-}B_{10}H_8\text{-}1,10\text{-}(NH_2)_2]^{2-}$. Experimental details have not been published.
(82) A reaction of $[closo\text{-}B_{10}H_8\text{-}1,10\text{-}(NH_2)_2]^{2-}$ $2Na^+$ prepared in situ in diglyme with NOCl was reported in ref 43 to give $[closo\text{-}B_{10}H_8\text{-}1,10\text{-}(N_2)_2]$ in a low yield.

Scheme 7

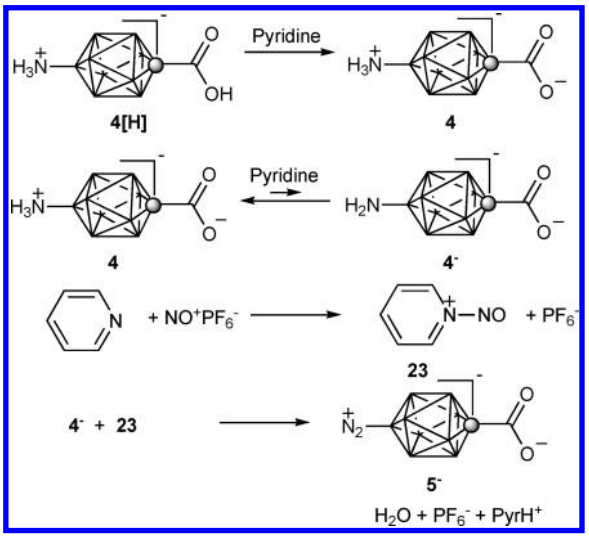

The reaction of $NO^+PF_6^-$ with **4**[**H**] in the presence of pyridine is a complex process in which the base serves a dual role: it deprotonates the NH_3 group and presumably reacts with $NO^+PF_6^-$ to form an alternative diazotizing reagent, the *N*-nitrosopyridinium ion[83,84] (**23**). It can be postulated that the formation of **5** involves initial deprotonation of the COOH group in **4**[**H**] and subsequent proton-transfer equilibrium between the NH_3^+ group and pyridine (Scheme 7). On the basis of the measured p*K* values, the equilibrium is significantly shifted to the left and the required ambident anion $\mathbf{4}^-$ is present in low concentrations. The subsequent addition of $NO^+PF_6^-$ leads to the formation of cation **23**. Although, the ambident ion **4** may compete with pyridine for NO^+, the green color[85] developing immediately upon addition of a portion of $NO^+PF_6^-$ to the solution and fading to clear/yellowish suggests that cation **23** is formed preferentially and serves as the main diazotizing reagent for $\mathbf{4}^-$. The reaction requires excess $NO^+PF_6^-$, since at least 1 equiv is presumably consumed by water formed during diazotization.

The reactivity of the B(10) dinitrogen acid **5** is distinctly different from that of C(1) dinitrogen derivative **17**.[50] Unlike dinitrogen species **17**, where identical reactions with nucleophiles occur at ambient temperature,[50] reactions of dinitrogen acid **5** require heating to about 100 °C. The observed relatively high thermal stability of **5** is consistent with behavior of apical dinitrogen derivatives of the $[closo\text{-}B_{10}H_{10}]^{2-}$ cluster.[40−49]

The most striking difference in reactivity of the C(1) and B(10) dinitrogen derivatives is, however, the regioselectivity of their reactions with pyridine. While the former (**17**) gives a mixture of C-substituted pyridines as the sole products,[50] reactions of **5** with hot pyridine leads to the exclusive formation of the *N*-isomer, pyridine acid **6**. The formation of **6** is consistent with reactions of other *B*-dinitrogen derivatives of $[closo\text{-}B_{10}H_{10}]^{2-}$ with pyridine[42,43,45,86] (Figure 9).

(83) Olah, G. A.; Olah, J. A.; Overchuk, N. A. *J. Org. Chem.* **1965**, *30*, 3373–3376.
(84) Lee, K. Y.; Kochi, J. K. *J. Chem. Soc. Perkin. Trans. 2* **1994**, 237–245.
(85) A similar green color was formed in a reaction between pyridine and $NO^+PF_6^-$ in the absence of **4**, and also reported in literature (see reference 83).
(86) Leyden, R. N.; Hawthorne, M. F. *Inorg. Chem.* **1975**, *14*, 2444–2446.

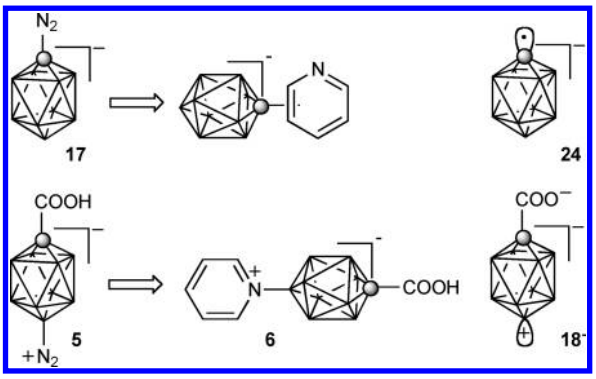

Figure 9. Regioselectivity of reaction of **5** and **17** with pyridine.

Table 4. Calculated Gas Phase Adiabatic Electron Affinity (E_a) and Experimental Electrochemical Reduction Potentials for Selected Compounds

	calculated[a]	experimental[b]	
compound	E_a /eV	$E_{1/2}^{red}$ /V	E_{pc}^{red}/V [c]
$C_6H_5N_2^+$	5.45	[d]	−0.16 [e,f]
[*closo*-1-CB_9H_9-1-N_2] (**17**)	2.06	[d]	−0.54 [e]
[*closo*-1-CB_9H_8-10-N_2-1-COOMe] (**11**)	1.00	−1.03 [g]	−1.10
[*closo*-1-CB_9H_9-10-N_2] (**16**)	0.60		
[*closo*-1-CB_9H_8-10-N_2-1-COO]$^-$ ($\mathbf{5}^-$)	−1.97	−1.21 [g]	−1.34

[a] MP2/6-31G(d,p) level with DFT enthalpic corrections. [b] Recorded in MeCN (0.05 M Bu_4NPF_6) versus SCE. [c] Peak potential. [d] Irreversible process. [e] Ref 50. [f] Lit. −0.17 (MeCN, SCE) ref 87. [g] Process partially reversible.

The observed diametrically different regioselectivities for the reactions of **5** and **17** are consistent with different mechanistic pathways and reactive intermediates involved in transformation of each dinitrogen derivative. Thus, for reactions of **17** we postulated[50] the nucleophile-induced formation of radical anion [*closo*-1-CB_9H_9]$^{-\bullet}$ (**24**, Figure 9) and its reaction with pyridine in accordance with the Gomberg−Bachmann mechanism for arylation with arenediazonium salts. The formation of the radical intermediates in this process requires dinitrogen precursors with high electron affinity (low reduction potential). Our previous experiments demonstrated that reduction of **17** is more cathodic than that of PhN_2^+ by about 0.4 V (Table 4), which apparently is still low enough for a nucleophile to trigger the radical ion mechanism for **17**.[50] In contrast, reduction of dinitrogen ester **11** is more difficult by 0.56 V than **17** or by nearly 1 V relative to PhN_2^+. This apparently renders the nucleophile-induced formation of radical too slow for effective competition with the alternative process involving boronium ylide. Deprotonation of the dinitrogen acid **5** in pyridine solutions increases further the reduction potential to $E_{1/2} = -1.25$ V, which makes the electron transfer from the nucleophile even more unfavorable, and at the same time the heterolytic cleavage of the B−N bond and the formation of the ylide $\mathbf{18}^-$ is predicted to be easier (Table 2).

Finally, a comment on the relative stability of the 1- and 10- isomers. Calculations indicate that the B(10) isomers are significantly more thermodynamically stable that the C(1) analogues (Table 5). For the pairs of compounds in Table 5

Table 5. Relative Thermodynamic Stability for Selected Pairs of Isomers[a]

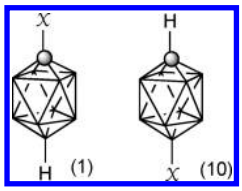

X	$\Delta H = H_{(1)} - H_{(10)}$ [b] /kcal mol^{-1}
N_2 (**17** and **16**)	52.4
+ [c] (**20** and **19**)	44.6
Pyridinium (**22** and **21**)	38.9

[a] MP2/6-31G(d,p) level with DFT enthalpic corrections. [b] Difference in enthalpy of formation between the (1) and (10) isomers shown above. [c] Vacant orbital in ylides.

the calculated difference in the enthalpy of formation is about 39 kcal/mol for the pyridinium derivatives **21** and **22**, and as high as 52.4 kcal/mol for the isomers **16** and **17** containing the strongly electron withdrawing dinitrogen substituent. The calculated high stability of the B(10)−N_2 isomer is consistent with the experimental results and appears to be general for apical derivatives of the [*closo*-$B_{10}H_{10}$]$^{2-}$ cluster; similarly to **5** and **11** they are isolable stable compounds[40,42,43,68,86,88] and serve as important intermediates in the preparation of a variety of derivatives of the {*closo*-B_{10}} cluster. The higher stability of the B−N_2 versus C−N_2 isomer is consistent with the UV spectra indicating a higher HOMO−LUMO gap because of lower charge separation of the B−N bond as compared to the C−N analogue.

Summary and Conclusions

A practical and reproducible method for converting iodo acid **1**[**NMe$_4$**] to amino acid **4**[**NMe$_4$**] and subsequently to stable dinitrogen acid **5** has been developed. The latter undergoes thermolysis at about 100 °C and forms boronium ylide **18**, which is efficiently trapped by a nucleophilic solvent. The synthetic utility of this reaction was demonstrated with high yield preparation of pyridinium acid **6** and protected mercapto acid **7**. Experimental results and theoretical analysis showed that the B(10) dinitrogen derivatives, such as **5**, are less electrophilic and more thermodynamically stable than the isomeric C(1) dinitrogen derivatives, such as **17**. Therefore, the former derivatives react solely through the heterolytic cleavage of the B(10)−N bond and boronium ylide intermediates. In contrast, the C(1)−N_2 derivatives undergo nucleophile-induced homolytic cleavage of the C−N bond, which leads to radical anion formation. The two distinct mechanistic pathways result in different regiochemical outcome of reaction of **5** and **17** with pyridine.

Computational results indicate that the reactivity of the dinitrogen derivatives and the stability of the resulting boronium ylides can be controlled to some extent by antipodal substituents at the C(1) vertex.

Overall, the demonstrated Pd-catalyzed transformations of iodo acid **1** (alkylation and amination) and access to amino acid **4**[**NMe$_4$**] open new opportunities for the incorporation of the [*closo*-1-CB_9H_{10}]$^-$ cluster into more complex molecular architectures, such as anisometric molecules. Our current work concentrates on applying this methodology in

(87) Andrieux, C. P.; Pinson, J. *J. Am. Chem. Soc.* **2003**, *125*, 14801–14806.

(88) Knoth, W. H. *J. Am. Chem. Soc.* **1972**, *94*, 104–109.

the development of polar liquid crystalline materials for electro-optical applications.

Computational Details

Quantum-mechanical calculations were carried out with the B3LYP[89,90] and MP2(fc)[91] methods with the 6-31G(d,p) basis set using the Gaussian 03 package.[92] Geometry optimizations were undertaken using appropriate symmetry constraints and tight convergence limits. Vibrational frequencies were used to characterize the nature of the stationary points and to obtain thermodynamic parameters. Zero-point energy (ZPE) corrections were scaled by 0.9806.[93] Hybridization parameters and natural charges were obtained using the NBO algorithm supplied in the Gaussian 03 package.[92] Population analysis of the MP2 wave function (MP2//MP2) was performed using the DENSITY(MP2) keyword. The IPCM solvation model[94] was used with default parameters and $\varepsilon = 52.5$ for EtOH/H_2O (1:1, v/v) at 25 °C, which was interpolated from the reported values for EtOH/H_2O mixtures.[95]

Excitation energies for derivatives of the {*closo*-1-CB_9} cluster were obtained at their MP2 determined geometries using the INDO/2 algorithm (ZINDO)[96] as supplied in Cerius2 suite of programs and including all electrons and orbitals in the CI. ZINDO calculations with the solvation model (Self Consistent Reaction Field) used cavity radii derived from the MP2 calculations with the VOLUME and DENSITY(MP2) keyword. The list of used cavity radii is provided in the Supporting Information.

Experimental Section

Reagents and solvents were obtained commercially. Pyridine was distilled from KOH and stored over 4 Å molecular sieves. *N*,*N*-dimethylthioformamide was distilled (80 °C, 0.25 mmHg) prior to use. All other reagents were used as supplied. Reactions were carried out under Ar, and subsequent manipulations were conducted in air. NMR spectra were obtained at 128.4 MHz (^{11}B) and 400.1 MHz (^{1}H) in CD_3CN or CD_3OD as specified. ^{1}H NMR spectra were referenced to the solvent, and ^{11}B NMR chemical shifts were referenced to an external boric acid sample in CH_3OH that was set to 18.1 ppm. IR spectra were recorded in the solid state using an AT-IR accessory. Ultraviolet absorption spectra were recorded in Optima grade CH_3CN.

Temperature-Dependent NMR Study of the Decomposition of 11 in Benzonitrile. The temperature-dependent NMR kinetic study of [*closo*-1-CB_9H_8-1-COOMe-10-N_2] (**11**) was performed on a 400 MHz NMR at 140 °C, 135 °C, 130 °C, and 125 °C in nondeuterated PhCN, which was dried over 4 Å molecular sieves for 24 h before use. Each experiment was performed with 5 mg of **11** dissolved in 0.6 mL of PhCN. A NMR tube filled with an equivalent volume of PhCN was used for tuning and shimming (1D) at the desired temperature. ^{11}B-{^{1}H} NMR experiments were executed using a time-delay controlled by the NMR console of 113.26 s. Each experiment consisted of 128 scans to improve resolution and reduce baseline noise. For experiments at 140 and 135 °C, each data point reflects one experiment whereas two experiments were recorded for each data point at 130 and 125 °C.

Dissociation Constant p*K* Measurements. Apparent dissociation constants were determined for **4**[NMe_4], **9**[NEt_4], and benzoic acid by potentiometric titration at 24 °C. The pH of the half-equivalent point at which [HA] = [A^-] was taken as the apparent p*K* of the acid HA as described in the Henderson−Hasselbach equation.[62,97] No corrections for solvent effect (e.g., for 50% aqueous ethanol a correction of $\Delta pK_a = +0.23$ is recommended)[98] or ion activity were made. Selected compound was dissolved in EtOH/H_2O (1:1 vol/vol, ∼0.01 M) and covered with parafilm to minimize evaporation of solvent. Neutralization was achieved under stirring with 0.05 M NaOH or 0.05 M HCl in EtOH/H_2O (1:1, vol/vol), which was added in 50 μL increments using a digital pipet. The pH electrode was calibrated in aqueous buffer (pH = 4.0, 7.0, and 10.0) followed by soaking in EtOH/H_2O (1:1 vol/vol) for 4 h or until the pH reading stabilized. After addition of titrant, the pH was recorded upon stabilization (∼30 s). For **9**[NEt_4] and benzoic acid two titrations gave p*K* values within 0.01. The pK_2 for **4**[NMe_4] was obtained as an average of 4 titrations (5.61 ± 0.08).

Electrochemical Measurements. Electrochemical analysis was conducted in dry, degassed (with Ar) MeCN with Bu_4NPF_6 (0.05 M) as the supporting electrolyte using a freshly polished glassy carbon working electrode with the Ag/AgCl reference electrode. The scanning rate was 1 V/s. Following literature recommendations,[87] the concentration of compounds **11** and **5**$^-$[NMe_4] was set at 0.6 mM and the reported data was taken from the first scan. Continuous scanning of the electrochemical window (+0.8 to −2.0 V) resulted in little shifting of the observed cathodic and anodic peak potentials, which suggests no surface modification of the electrode surface by products of the initial reduction process. Peak potentials were referenced by adding small amounts of ferrocene to the solution and E-chem scans for each compound were referenced to the ferrocene couple which was assumed to be 0.31 V versus SCE (MeCN, 0.2 M $LiClO_4$)[99] or 0.35 V vrs Ag/AgCl electrode.

Preparation of [*closo*-1-CB_9H_8-1-COO-10-NH_3]$^-$$NMe_4^+$ (4[NMe_4]). [*closo*-1-CB_9H_8-1-COOH-10-I]$^-$$NMe_4^+$ (**1**[NMe_4], 1.00 g, 2.75 mmol) was added to a solution of lithium hexamethyldisilazane (LiHMDS, 41.2 mL, 41.3 mmol, 1.0 M in THF) at room temperature (rt) under Ar. The light orange suspension was stirred vigorously for 15 min or until the suspension became more fine and disperse. Pd_2dba_3 (0.050 g, 0.055 mmol) and 2-(dicyclohexylphosphino)biphenyl (0.077 g, 0.22 mmol) were added, and the reaction was stirred at reflux for 20 h. After several minutes at reflux, the reaction mixture turned dark brown. The reaction was cooled to 0 °C, and 10% HCl

(89) Becke, A. D. *J. Chem. Phys.* **1993**, *98*, 5648–5652.
(90) Lee, C.; Yang, W.; Parr, R. G. *Phys. Rev. B* **1988**, *37*, 785–789.
(91) Møller, C.; Plesset, M. S. *Phys. Rev.* **1934**, *46*, 618–622. Head-Gordon, M.; Pople, J. A.; Frisch, M. J. *Chem. Phys. Lett.* **1988**, *153*, 503–506.
(92) Frisch, M. J.; Trucks, G. W.; Schlegel, H. B.; Scuseria, G. E.; Robb, M.; Cheeseman, J. R.; Montgomery, J. A.; Vreven, J. A.; Kudin, K. N.; Burant, J. C.; Millam, J. M.; Iyengar, S. S.; Tomasi, J.; Barone, V.; Mennucci, B.; Cossi, M.; Scalmani, G.; Rega, N.; Petersson, G. A.; Nakatsuji, H.; Hada, M.; Ehara, M.; Toyota, K. ; Fukuda, R.; Hasegawa, J.; Ishida, M.; Nakajima, T.; Honda, Y.; Kitao, O.; Nakai, H.; Klene, M.; Li, X.; Knox, J. E.; Hratchian, H. P.; Cross, J. B.; Adamo, C.; Jaramillo, J; Gomperts, R.; Stratmann, R. E.; Yazyev, O.; Austin, A. J.; Cammi, R.; Pomelli, C.; Ochterski, J. W.; Ayala, P. Y.; Morokuma, K.; Voth, G. A.; Salvador, P.; Dannenberg, J. J.; Zakrzewski, V. G.; Dapprich, S.; Daniels, A. D.; Strain, M. C.; Farkas, O.; Malick, D. K.; Rabuck, A. D.; Raghavachari, K.; Foresman, J. B.; Ortiz, J. V.; Cui, Q. ; Baboul, A. G. ; Clifford, S. ; Cioslowski, J.; Stefanov, B. B.; Liu, G.; Liashenko, A.; Piskorz, P.; Komaromi, I.; Martin, R. L.; Fox, D. J.; Keith, T.; Al-Laham, M. A.; Peng, C. Y.; Nanayakkara, A.; Challacombe, M.; Gill, P. M. W.; Johnson, B.; Chen, W.; Wong, M. W.; Gonzalez, C.; Pople, J. A. *Gaussian 03*, Revision D.01; Gaussian, Inc.: Wallingford, CT, 2004.
(93) Scott, A. P.; Radom, L. *J. Phys. Chem.* **1996**, *100*, 16502–16513.
(94) Foresman, J. B.; Keith, T. A.; Wiberg, K. B.; Snoonian, J.; Frisch, M. J. *J. Phys. Chem.* **1996**, *100*, 16098–16104.
(95) Hasted, J. B. In *Water a Comprehensive Treatise*; Franks, F., Ed.; Plenum Press: New York, 1973; Vol *2*, p 421.
(96) Zerner, M. C. In *Reviews of Computational Chemistry*; Lipkowitz, K. B., Boyd, D. B., Eds.; VCH Publishing: New York, 1991; Vol. *2*, pp 313−366, and references therein.
(97) Albert, A.; Serjeant, E. P. *The Determination of Ionization Constants: A Laboratory Manual*, 2nd ed.; Chapman and Hall Ltd: London, 1971.
(98) Rubino, J. T.; Berryhill, W. S. *J. Pharm. Sci.* **1986**, *75*, 182–186.
(99) Bard, A. J.; Faulkner, L. R. *Electrochemical Methods: Fundamentals and Applications*, 2nd ed.; Wiley: Hoboken, NJ, 2001.

(100 mL) was added slowly. The THF was removed in vacuo giving a dark orange solution. The orange solution was extracted with Et_2O (3 × 30 mL), the Et_2O layers were combined, dried (Na_2SO_4), and evaporated at slightly elevated temperature (~40 °C) to ensure complete removal of trimethylsilanol. ^{11}B NMR of the crude material revealed a 70:30 ratio of amino acid **4**[**H**] to parent acid **9**[**H_3O**].

The crude brown/orange material was redissolved in Et_2O, and H_2O (10 mL) was added. The Et_2O was removed in vacuo until bubbling became less vigorous. The aqueous layer was filtered, and the process was repeated two more times (the insoluble material presumably contains a B(10)-phosphonium derivative). The aqueous layers were combined, and $NEt_4^+Br^-$ (0.578 g, 2.75 mmol) was added resulting in precipitation of a white solid. CH_2Cl_2 (20 mL) was added, and the biphasic system was stirred vigorously until the H_2O layer became clear (~30 min). The CH_2Cl_2 was separated, and the process was repeated once more. The H_2O layer was filtered, reacidified with conc. HCl (5 mL), and extracted with Et_2O (3 × 10 mL). The Et_2O layers were combined, washed with H_2O, dried (Na_2SO_4), and evaporated giving 0.260 g of amino acid [*closo*-1-CB_9H_8-1-COOH-10-NH_3] (**4**[**H**]) with purity >90% by ^{11}B NMR.

Crude amino acid [*closo*-1-CB_9H_8-1-COOH-10-NH_3] (**4**[**H**], 0.194 g, 1.08 mmol) was dissolved in CH_3OH (5 mL), and $NMe_4^+OH^-\cdot 5H_2O$ (0.180 g, 0.993 mmol,) was added. The mixture was stirred for 1 h, CH_3OH was removed in vacuo, and the residue was washed with Et_2O and then with boiling MeCN (2×) to give 0.221 g (88% recovery, 44% overall yield) of pure amino acid [*closo*-1-CB_9H_8-1-COO-10-NH_3]$^-NMe_4^+$ (**4**[**NMe_4**]) as a fluffy off-white solid: mp >260 °C; ^1H NMR (CD_3OD) δ 0.5−2.4 (br m, 8H), 3.19 (s, 12H), resonance for N*H*$_3$ was not observed; ^{11}B NMR (CD_3OD) δ −22.8 (d, J = 155 Hz, 4B), −17.4 (d, J = 149 Hz, 4B), 34.7 (s, 1B); IR 3400−2800 br (N−H), 2539 (B−H), 1555 and 1383 cm^{-1}. Anal. Calcd for $C_6H_{23}B_9N_2O_2$: C, 28.53; H, 9.18; N, 11.09. Calcd for $C_6H_{23}B_9N_2O_2\cdot H_2O$: C, 26.63; H, 9.31; N, 10.35. Found: C, 26.88; H, 9.43; N, 10.10.

Preparation of [*closo*-1-CB_9H_8-1-COOH-10-NH_3] (4[H]). Amino acid [*closo*-1-CB_9H_8-1-COO-10-NH_3]$^-NMe_4^+$ (**4**[**NMe_4**], 0.055 g, 0.22 mmol) was dissolved in 10% HCl (2 mL), and the solution was extracted with ether (3 × 2 mL). The organic layers were combined, washed with H_2O (2 mL), dried (Na_2SO_4), and the solvent evaporated. The white solid residue was dried in vacuum to give 0.039 g (~100% yield) of pure acid [*closo*-1-CB_9H_8-1-COOH-10-NH_3] (**4**[**H**]) as a white solid: mp >260 °C; ^1H NMR (CD_3CN) δ 0.5−2.4 (m, 8H), 6.6 (br t, J = 37 Hz, 3H), 9.6 (brs); (CD_3OD) δ 0.5−2.4 (m, 8H), 7.8 (br s, 1.2H); ^{11}B NMR (CD_3CN) δ −22.6 (d, J = 141 Hz, 4B), −16.8 (d, J = 158 Hz, 4B), 37.0 (s, 1B); (CD_3OD) δ −22.6 (d, J = 152 Hz, 4B), −16.8 (d, J = 145 Hz, 4B), 38.1 (s, 1B); IR 3300−2800 br (N−H and O−H), 2571 (B−H), 1671 (C═O) cm^{-1}; FAB-HRMS(-), calcd. for $C_2H_{10}B_9NO_2$ m/z: 179.1549; found: 179.1534.

Preparation of [*closo*-1-CB_9H_8-1-COOH-10-N_2] (5). Amino acid [*closo*-1-CB_9H_8-1-COOH-10-NH_3] (**4**[**H**], 0.105 g, 0.59 mmol) was suspended in anhydrous CH_3CN (2 mL) under Ar. Anhydrous pyridine (0.240 mL, 2.93 mmol) was added, and the mixture was sonicated for 5 min. The reaction mixture was cooled to −15 °C, and nitrosonium hexafluorophosphate ($NO^+PF_6^-$, 0.310 g, 1.77 mmol) was added in five portions at 5 min intervals. Addition of $NO^+PF_6^-$ resulted in a green/blue homogeneous solution that slowly faded to colorless, and the solution became more yellow as more $NO^+PF_6^-$ was introduced. Once all $NO^+PF_6^-$,was added, the reaction was stirred for 1.5 h at −15 °C.

The reaction mixture was evaporated to dryness (the flask was kept at cold water bath), 10% HCl (10 mL) was added, and the mixture was stirred vigorously until all solids had dissolved (~20 min). The aqueous solution was extracted with Et_2O (3 × 5 mL), the Et_2O layers were combined, washed with H_2O, dried (Na_2SO_4), and evaporated to dryness giving 0.107 g of crude dinitrogen acid **5**. The crude product was passed through a short silica gel plug (CH_3OH/CH_2Cl_2, 1:19, R_f = 0.2) giving 0.087 g (78% yield) of dinitrogen acid [*closo*-1-CB_9H_8-1-COOH-10-N_2] (**5**) as a white solid, which was recrystallized from aqueous MeOH containing a few drops of acetone: mp 174−177 °C dec; ^1H NMR (CD_3CN) δ 1.0−2.7 (br m, 8H), 10.0 (br s, 1H); ^{11}B NMR (CD_3CN) δ −15.5 (d, J = 158 Hz, 4B), −13.6 (d, J = 169 Hz, 4B), 20.3 (s, 1B); IR 2291 (N_2) cm^{-1}; UV (CH_3CN), λ_{max} 216 nm (log ε = 4.33); FAB-HRMS(-), calcd. for $C_2H_9B_9N_2O_2$ m/z: 192.1502; found: 192.1501. Anal. Calcd for $C_2H_9B_9N_2O_2$: C, 12.62; H, 4.76; N, 14.71; Found: C, 13.06; H, 4.87; N, 14.58.

Preparation of [*closo*-1-CB_9H_8-1-COOH-10-(1-NC_5H_5)] (6). A slight yellow solution of [*closo*-1-CB_9H_8-1-COOH-10-N_2] (**5**, 0.048 g, 0.25 mmol) and anhydrous pyridine (3.0 mL, 37.1 mmol) was stirred at 100 °C for 1 h. As the reaction progressed, bubbling of N_2 became evident. Excess pyridine was removed in vacuo, 10% HCl (10 mL) was added to the residue, and the solution was extracted with Et_2O (3 × 5 mL). The Et_2O layers were combined, washed with H_2O, dried (Na_2SO_4), and evaporated giving 0.060 g of crude pyridinium acid **6** as a slight yellow solid. The crude product was passed through a short silica gel plug (CH_3OH/CH_2Cl_2, 1:19, R_f = 0.4) giving 0.054 g (90% yield) of acid [*closo*-1-CB_9H_8-1-COOH-10-(1-NC_5H_5)] (**6**) as an off-white solid, which was further purified by recrystallization from $EtOH/H_2O$ (3×): mp 258−260 °C; ^1H NMR (CD_3CN) δ 1.0−2.5 (br m, 8H), 8.03 (t, J = 7.2 Hz, 2H), 8.50 (t, J = 7.8 Hz, 1H), 9.31 (d, J = 5.2 Hz, 2H); ^{11}B NMR (CD_3CN) δ −20.9 (d, J = 131 Hz, 4B), −16.2 (d, J = 160 Hz, 4B), 42.2 (s, 1B); UV (CH_3CN), λ_{max} 264 nm, (log ε = 4.07); FAB-HRMS(+), calcd. for $C_7H_{14}B_9NO_2$ m/z: 243.1862; found: 243.1853. Anal. Calcd for $C_7H_{14}B_9NO_2$: C, 34.81; H, 5.84; N, 5.80. Found: C, 35.46; H, 5.86; N, 5.89.

Preparation of [*closo*-1-CB_9H_8-1-COOH-10-SCHN(CH_3)$_2$] (7). A solution of [*closo*-1-CB_9H_8-1-COOH-10-N_2] (**5**, 0.061 g, 0.32 mmol) and freshly distilled Me_2NCHS (3.0 mL, 35.2 mmol) was stirred at 100 °C for 1 h. As the reaction progressed, bubbling of N_2 became evident. Excess Me_2NCHS was removed by vacuum distillation (95 °C, 1.5 mmHg) leaving crude product as an off-white crystalline solid. The crude product was washed with toluene giving 0.076 g (95% yield) of crude protected mercaptan [*closo*-1-CB_9H_8-1-COOH-10-SCHN(CH_3)$_2$] (**7**) containing ~5% of Me_2NCHS by ^1H NMR: mp 250−253 °C dec; ^1H NMR major signals (CD_3CN) δ 0.6−2.5 (br m, 8H), 3.50 (s, 3H), 3.57 (s, 3H), 9.49 (s, 1H); minor signals for Me_2NCHS: δ 3.19 (s, 3H), 3.25 (s, 3H), 9.12 (s, 1H); ^{11}B NMR (CD_3CN) major signals δ −20.4 (d, J = 144 Hz, 4B), −15.3 (d, J = 155 Hz, 4B), 35.2 (s, 1B); FAB-HRMS(+), calcd. for $C_5H_{16}B_9NO_2S$ m/z: 253.1739; found: 253.1734.

Preparation of [*closo*-1-CB_9H_8-1-COOH-10-(1-SC_5H_{10})] (8). A solution of crude protected mercaptan [*closo*-1-CB_9H_8-1-COOH-10-SCHN(CH_3)$_2$] (**7**, 0.065 g, 0.26 mmol) in anhydrous CH_3CN (4 mL) was treated with a solution of $NMe_4^+OH^-\cdot 5H_2O$ (0.236 g, 1.3 mmol) in anhydrous CH_3CN (6 mL) resulting in the formation of a white precipitate. 1,5-Dibromopentane (36 μL, 0.26 mmol) was added, and the reaction mixture was stirred for 24 h at rt. The reaction mixture was evaporated to dryness and stirred in a methanol solution (4 mL) of NaOH (0.01 g, 0.250 mmol) at 50 °C for 4 h, to hydrolyze small amounts of ester. Solvent was removed to dryness and 10% HCl (10 mL) was added. The suspension was stirred vigorously with Et_2O (5 mL) until the aqueous layer became homogeneous. The Et_2O layer was separated, and the aqueous layer was further extracted with Et_2O (2 × 5 mL). The Et_2O layers were combined, washed with H_2O, dried (Na_2SO_4), and evaporated leaving 0.064 g of crude sulfonium acid **8** as an orange crystalline film. The crude material was passed through a short silica gel plug (CH_3OH/CH_2Cl_2, 1:19, R_f = 0.4) and washed with hot hexane giving 0.037 g 54% yield) of

[*closo*-1-CB_9H_8-1-COOH-10-(1-SC_5H_{10})] (**8**) as an off-white solid. The product was recrystallized from aq EtOH and then from toluene to give colorless blades of acid **8** as a solvate with toluene (1:1). The solvent was removed by heating at 100 °C in vacuum for 2 h: mp 232−233 °C; ^{1}H NMR (CD_3CN) δ 0.6−2.5 (br m, 8H), 1.60−1.75 (m, 2H), 1.93−2.05 (m, 2H), 2.29−2.33 (m, 2H), 3.36 (td, J_1 = 12.2 Hz, J_2 = 2.4 Hz, 2H), 3.66 (dm, J = 12.4 Hz, 2H), 9.71 (brs, 1H); ^{11}B NMR (CD_3CN) δ −20.2 (d, J = 149 Hz, 4B), −14.8 (d, J = 160 Hz, 4B), 32.1 (s, 1B); FAB-HRMS(+), calcd. for $C_7H_{19}B_9O_2S$ m/z: 266.1943; found: 266.1933.

Preparation of [*closo*-1-CB_9H_8-1-COOMe-10-NH_3] (10[H]). A suspension of [*closo*-1-CB_9H_8-1-COOH-10-NH_3] (**4**[**H**], 0.025 g, 0.14 mmol) in anhydrous CH_2Cl_2 (2 mL) containing $(COCl)_2$ (0.15 mL, 0.29 mmol, 2.0 M in CH_2Cl_2) was treated with anhydrous DMF (0.1 mL, 1.4 mmol). Intense bubbling ensued followed by dissolution of the substrate, and the reaction was stirred at rt for an additional 30 min. Solvents were removed to complete dryness leaving a light yellow residue of acid chloride [*closo*-1-CB_9H_8-1-COCl-10-NH_3]: ^{1}H NMR (CD_3CN) δ 8.38 (br t, J = 34 Hz); ^{11}B NMR (CD_3CN) δ −22.6 (d, J = 140 Hz, 4B), −15.3 (d, J = 158 Hz, 4B), 41.4 (s, 1B).

The crude chloride was dissolved in anhydrous CH_3OH (5 mL) and refluxed for 1 h. The reaction was evaporated to dryness, suspended in Et_2O (5 mL), and treated with 5% HCl (10 mL). The Et_2O layer was separated, and the aqueous layer was further extracted with Et_2O (2 × 5 mL). The Et_2O layers were combined, washed with H_2O, dried (Na_2SO_4), and evaporated to dryness giving 0.026 g (96% yield) of **10**[**H**] as slight yellow microcrystals: mp >260 °C; ^{1}H NMR (CD_3CN) δ 0.5−2.50 (br m, 8H), 3.92 (s, 3H), 6.58 (br t, J = 42 Hz, 3H) [^{1}H-{^{14}N} 6.57 (s, 3H)]; ^{11}B NMR (CD_3CN) δ −22.6 (d, J = 142 Hz, 4B), −16.8 (d, J = 156 Hz, 4B), 37.1 (s, 1B); IR 3277 and 3126 (N−H), 2569 (B−H), 1724 (C=O); ESI-HRMS (+) calcd. for $C_3H_{14}B_9NNaO_2$ m/z: 217.1798; found: 217.1778.

Preparation of [*closo*-1-CB_9H_8-1-COOMe-10-N_2] (11). A cooled solution (~0 °C) of [*closo*-1-CB_9H_8-1-COOH-10-N_2] (**5**, 0.028 g, 0.15 mmol) in anhydrous Et_2O (2.0 mL) and diazomethane (generated from 0.076 g, 0.74 mmol of *N*-methyl-*N*-nitrosourea) were stirred for 1 h. The reaction mixture was evaporated to dryness giving 42 mg of crude product as a white solid. The crude material was passed through a short silica gel plug (CH_2Cl_2, R_f = 0.5) giving 24 mg (78% yield) of [*closo*-1-CB_9H_8-1-COOMe-10-N_2] (**11**) as a white crystalline solid. An analytical sample was prepared by recrystallization from EtOH/H_2O (slow evaporation of EtOH): mp 132−134 °C dec; ^{1}H NMR (CD_3CN) δ 1.2−2.7 (br m, 8H), 3.97 (s, 3H); ^{11}B NMR (CD_3CN) δ −15.5 (d, J = 163 Hz, 4B), −13.6 (d, J = 169 Hz, 4B), 20.4 (s, 1B); IR 2611, 2588, and 2558 (B−H), 2296 (N_2), 1735 (C=O), 1321 (C−O) cm^{-1}; ESI-HRMS(+); calcd. for $C_3H_{11}B_9N_2NaO_2$ m/z: 229.1556; found: 229.1551. Anal. Calcd for $C_3H_{11}B_9N_2O_2$: C, 17.63; H, 5.42; N, 13.70; Found: C, 18.08; H, 5.60; N, 13.39.

Ester [*closo*-1-CB_9H_8-1-($COOC_6H_{11}$)-10-(1-NC_5H_5)] (12). A red/orange solution of pyridinium acid [*closo*-1-CB_9H_8-1-COOH-10-(1-NC_5H_5)] (**6**, 30 mg, 0.124 mmol), dry cyclohexanol (15 mg, 0.150 mmol), and 2-chloro-3,5-dinitropyridine (25 mg, 0.124 mmol) in anhydrous pyridine (2 mL) was stirred at reflux under Ar. The ratio of peaks at 5.07 ppm and 9.31 ppm in ^{1}H NMR (CD_3CN) was monitored until the desired 1:2. ratio was achieved. If the reaction was not complete, additional equivalents of alcohol and 2-chloro-3,5-dinitropyridine were added, and heating was continued. Excess pyridine was removed to dryness giving a red/orange crystalline film. The film was treated with 10% HCl and extracted into Et_2O (3×). The Et_2O layers were combined, washed with H_2O, dried (Na_2SO_4), and evaporated to dryness. The crude product was further purified by passing through a short silica gel plug (hexane/CH_2Cl_2; 3:7). The eluent was filtered through a cotton plug, and the product was recrystallized (5×) from iso-octane/toluene mixtures in the freezer. Ester **12** was obtained in 75% yield as colorless blades (R_f = 0.5 in CH_2Cl_2): mp 175−177 °C; ^{1}H NMR (CD_3CN) δ 0.8−2.5 (br m, 8H), 1.30−1.69 (m, 6H), 1.73−1.83 (m, 2H), 1.90−2.03 (m, 2H), 5.07 (tt, J_1 = 8.6 Hz, J_2 = 3.8 Hz, 1H), 8.02 (t, J = 7.2 Hz, 2H), 8.50 (t, J = 7.8 Hz, 1H), 9.31 (d, J = 5.3 Hz, 2H) and peaks of toluene at 2.32 (s, 1.5H), 7.12−7.26 (m, 2.5H); ^{11}B NMR (CD_3CN) δ −21.0 (d, J = 145 Hz, 4B), −16.3 (d, J = 158 Hz, 4B), 42.0 (s, 1B). Anal. Calcd for $C_{13}H_{24}B_9NO_2$: C, 48.25; H, 7.47; N, 4.33. Calcd for $C_{13}H_{24}B_9NO_2 \cdot 1/2C_7H_8$: C, 53.60; H, 7.63; N, 3.79. Found: C, 53.21; H, 7.64; N, 3.85.

Ester [*closo*-1-CB_9H_8-1-($COOC_6H_4OMe$)-10-(1-SC_5H_{10})] (13). The ester was prepared from sulfonium acid [*closo*-1-CB_9H_8-1-COOH-10-(1-SC_5H_{10})] (**8**) and *p*-methoxyphenol as described for **12**. The ratio of peaks at 3.82 ppm and 7.01 ppm in ^{1}H NMR (CD_3CN) was monitored until the desired 3:2 ratio was achieved. Ester **13** was isolated in 54% yield as colorless needles (R_f = 0.6 in CH_2Cl_2): mp 158−160 °C; ^{1}H NMR (CD_3CN) δ 0.7−2.7 (br m, 8H), 1.61−1.73 (m, 2H), 1.90−2.05 (m, 2H), 2.30−2.34 (m, 2H), 3.38 (td, J_1 = 12.2 Hz, J_2 = 2.2 Hz, 2H), 3.69 (br d, J = 12.6 Hz, 2H), 3.82 (s, 3H), 7.01 (d, J = 9.0 Hz, 2H), 7.22 (d, J = 9.0 Hz, 2H); ^{11}B NMR (CD_3CN) δ −20.1 (d, J = 140 Hz, 4B), −14.4 (d, J = 159 Hz, 4B), 33.0 (s, 1B). Anal. Calcd for $C_{14}H_{25}B_9O_3S$: C, 45.36; H, 6.80; Found: C, 45.63; H, 6.79.

Acknowledgment. We thank the undergraduate students Sarah Muller and Breanna Stein, and also to Mr. Matthew Casella, for technical assistance with the preparation of **1**[NMe_4]. This project was supported by the NSF Grants DMR-0606317 and DMR-0907542. B.R. thanks for support while visiting Academy of Sciences of the Czech Republic (NSF Grants CHE-0446688 and OISE-0532040). Z.J. was supported by Grant Contact (project ME857) and the Ministry of Education, Youth, and Sports of the Czech Republic (project LC523).

Supporting Information Available: Synthetic details and characterization data for compounds **5**[NMe_4], **10**[NMe_4], **15**, and **23**, kinetic details for thermolysis of **11**, full crystal data collection information for **5**, **6**, and **8**, details for ZINDO calculations, archive of MP2 equilibrium geometries for selected molecules. This material is available free of charge via the Internet at http://pubs.acs.org.